Synthetic and Botanical Mosquito Repellent and their Antimicrobial Activity in PAN Membrane

Thesis submitted towards the partial fulfilment of
BS-MS dual degree programme

By

VIVEK VERMA
20091075

Under the guidance of
Dr. Balasubramanian K.
Associate Professor
Department of Materials Engineering
DIAT (DU), Pune

CERTIFICATE

This is to certify that this dissertation entitled "**Synthetic and Botanical Mosquito Repellent and their Antimicrobial Activity in PAN Membrane**" towards the partial fulfilment of the BS-MS dual degree programme at the Indian Institute of Science Education and Research, Pune represents original research carried out by Vivek Verma at Defence Institute of Advance Technology (DIAT), Pune under the supervision of Dr. Balasubramanian K., Associate Professor, HOD Department of Materials Engineering during the academic year 2013-2014.

Date:

Place: Signature

DECLARATION

I hereby declare that the matter embodied in the report entitled "**Synthetic and Botanical Mosquito Repellent and their Antimicrobial Activity in PAN Membrane**" are the results of the investigations carried out by me at the Department of Materials Engineering, DIAT (DU), Pune, under the supervision of Dr. Balasubramanian K. and the same has not been submitted elsewhere for any other degree.

Date:

Place: Signature

ACKNOWLEDGEMENT

It is a pleasure to thank those who made this thesis possible. First and foremost, I would like to thank my advisor **Dr. Balasubramanian K.** for his immense support and guidance. I feel privileged to be among his students. He celebrates research in the truest sense of the term. I would also like to thank him for providing us with such an excellent opportunity, and also for his encouragement throughout the duration of the project. Despite his busy schedule, he always found time to discuss with me and guides me throughout the project. His guidance has been an extraordinary learning experience. I also thank my co-advisor **Dr. Harinath Chakrapani** for his time to time encouragement and help throughout the year. I also thank **Dr. Shaibal Banerjee** (DIAT, Pune)for time to time help in chemistry throughout the year and **Dr. A. Sen** (NCL Pune) for characterization testing.

I would like to express my sincere gratitude to **Dr. Prahlada**, Vice Chancellor DIAT Pune for the state-of-the-art amenities and instrumentation in DIAT, Pune and **Dr. K. N. Ganesh**, Director, IISER Pune for giving me an opportunity to do my final year project outside IISER Pune campus and explore other labs.

I thank all my lab mates Bichitra, Renuka, Sanoj, Premika, Jitendra, Neha, Yutika, T. Manoj, Vijay, Navdeep for making the memories in room no. 130 & 131 fond and special. They provided me with the insight, constant help throughout the project and answered all my questions patiently. This place has left a lasting impression in me. This has been undoubtedly the best environment I have studied in and the above people were responsible for it.

Last but not the least; I owe my deep sense of gratitude to my family and friends as they have been very supportive throughout my life during the good and hard times.

-Vivek

CONTENTS

List of Figures and Tables

Abstract

Mosquito repellent plays a significant role in reducing bites and thereby extenuating transmission of mosquitoe-borne disease. The purpose of this thesis is also same i.e. to synthesize some mosquito repellents and also to discover botanical repellent. Pyruvic acid (one of the body emanation) was coupled with carboxamide containing moiety to form Pyr-ADB-dialkyl derivatives as mosquito repellents. Pyr-ADB-diisopropyl showed 8 h of repellency against *Aedes aegypti* mosquito specie with minimum effective dose (MED) of 0.5 mg/cm^2. *Lantana camara* oil (botanical repellent) also showed 8.5 h of repellency against the same mosquito specie at MED of 1.5 mg/cm^2. Lantana oil is also an effective antimicrobial agent hence its antimicrobial efficacy was examined immobilizing oil into polyacrylonitrile (PAN) membrane. Membrane showed excellent antibacterial activity against both gram-positive *Bacillus subtilis* and gram-negative *Escherichia coli* with a 7-10 mm zone of inhibition. *In vitro* release of *Lantana* oil from the composite membrane was carried out in isotonic phosphate buffer solution (pH=7.4). *Lantana* oil was released for 9 h, lag time of 3 h with constant 33% release confirmed PAN membranes as potential system for pulsatile drug delivery applications. Diffusion of E-caryophyllene (antibacterial component of oil) was studied through molecular simulation using Material Studio software ensued diffusion coefficient value of $1.11*10^{-9}$ m^2/s. Biocompatibility of the composite membrane was assessed by mouse embryonic fibroblasts cell line (NIH 3T3) through MTT assay indicating more than 91% viable cell even at 200 µg/mL concentration. Such membranes can be efficiently used in biomedical applications as antibacterial agent.

1. INTRODUTION

There are more than one million animals in the world, of which 80% are arthropods, and insects account for 90% of the arthropods. The arthropods were the first animals to exhibit joint appendages. Arthropods are amongst the most diverse phylum of animals, each subphylum is further divided into numerous classes. These appendages are modified into various types of antennae, mouthparts and legs. Insect belonging to arthropod phylum are mosquitoes (*Anopheles, Aedes, Culex*), biting midges (*Culicoides*), Sanflies (*Phlebotomus* or *Lutzomyia*), blackflies (*Simulium damnosum*), tsetse flies (*Glossina palpalis* group), body lice (*Pediculus humanus*), Fleas (*Pulex irritans*), bed bug (*Cimex lectularius*), kissing bugs (*Triatoma protracta*) etc. Insects of medicinal interest are numerous, and some have had a major impact on the course of human history due to epidemics of vector-borne diseases which have led to great effects on the health of human beings [1]. Insect vectors are responsible for the spread of serious human diseases such as leishmaniasis, river blindness, Chagas disease, sleeping sickness, typhus trench fever, bubonic plague.

There are more than 3000 species of mosquitoes, which belongs to 37 genera joined together in a single family: Culicidae. In countries with a temperate climate they are more important as nuisance pests than as vectors. Human biting mosquitoes are the most important vector of diseases belong to the genera *Anopheles, Culex, Aedes, Mansonia, Haemagogus* and *Sabethes* as shown in figure 1 [2]. Mosquitoes are the important vectors of several tropical diseases responsible for serious human diseases such as malaria, Japanese encephalitis, yellow fever, Rift Valley fever, and filariasis as well as dengue that cause severe mortality and morbidity in humans and livestock in the world [3].

Mosquitoes have four different stages in their life cycle: egg, larva, pupa and adult. Depending on the species, a female lay between 30 and 300 eggs at a directly on the surface of water either singly (*Anopheles*) or stuck together in floating rafts (*Culex*). Once hatched, the larvae grow in four different stages called instars. First instar larvae measures 1.5 mm in length while fourth instar measures 8-10 mm in length. Most mosquito larvae come to water surface to breathe through siphon located at the tip of the abdomen.

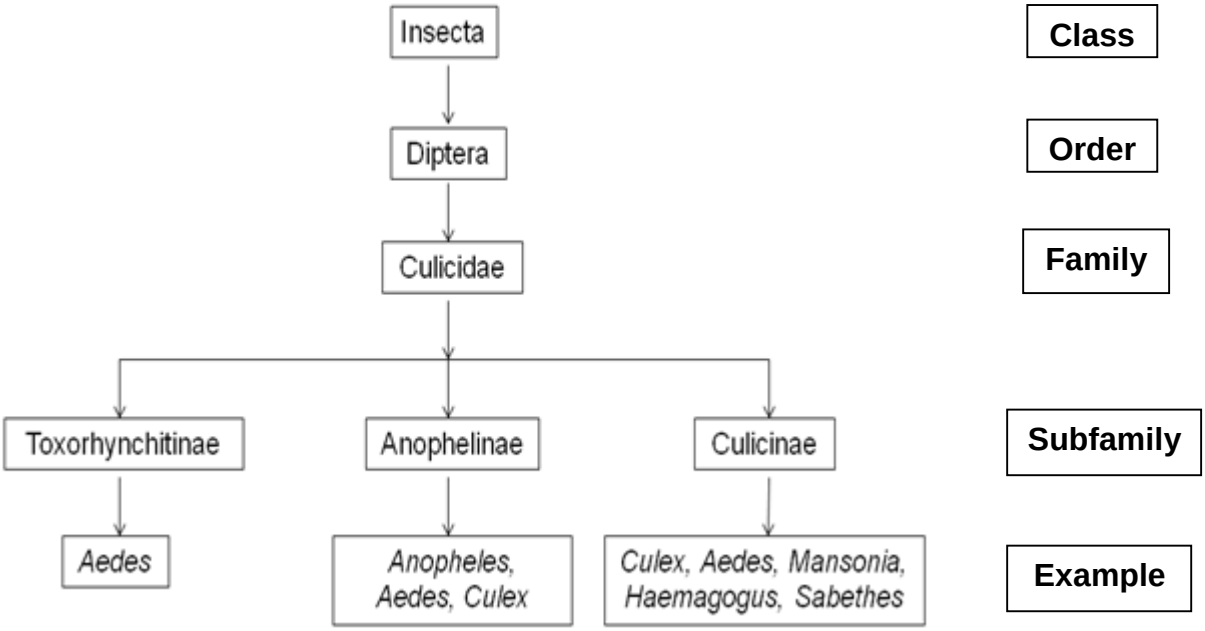

Figure 1: Insecta classification

Anopheles larvae feed and breathe horizontally at the surface because of rudimentary siphon while *Mansonia* larvae do not come to the surface as they breathe by inserting siphon into a water plant to which they remain attached most of the time. Fully grown larvae converts to comma shaped pupa and upon maturation pupal skin splits at one end and the fully grown mosquito emerges as shown in figure 2 [4].

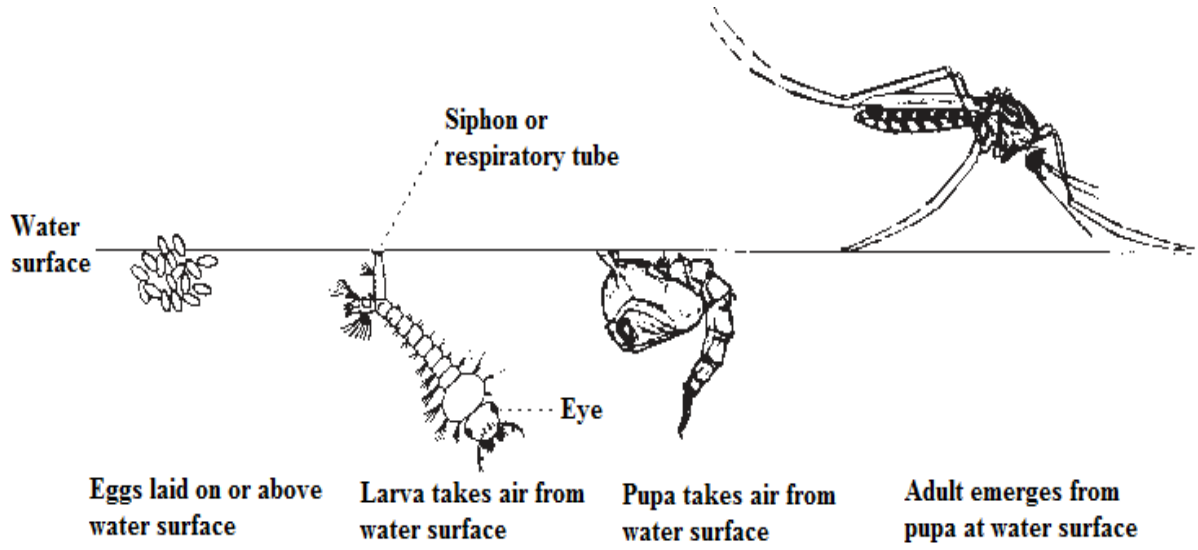

Figure 2: The life cycle of the mosquito [4]

1.1 Types of Mosquitoes

There are three subfamilies of the Culicidae family; *Culicinae, Anophelinae* and *Toxorhynchites*

1.1.1 Culicinae

Culicinae subfamily includes 33 genera and the most important ones in medical entomology are *Culex, Aedes, Mansonia, Haemagogus* and *Sabethes. Aedes, Culex* and *Mansonia* are the habitants of temperate and tropical region while *Sabethes* and *Haemagogus* are the habitants of Central and South America.

1.1.1.1 Culex

There are 800 species of *Culex* (Figure 3(b)) divided into 21 sub-genera mostly found in tropical and subtropical regions. Some species are important vectors of bancroftian filariasis and arboviral diseases such as Japanese encephalitis [5]. They breed specially in water polluted with organic materials, such as refuse and excreta of rotting plant. In many developing countries *Culex quinquefasciatus* is common anarchistic urbanization, with poor hygiene conditions and worn out water drainage and sanitation system. They have nocturnal activity with an endophilic tendency. The adult females bite people and animals throughout the night, indoors and outdoors while during day time they are inactive and found resting in dark corners of room, shelter and culverts.

1.1.1.2 Aedes

There are more than 800 species of *Aedes* (Figure 3(a)) divided in 36 subgenera and are widespread throughout the world. In tropical countries *Aedes aegypti* is the main vector of yellow fever while *Aedes albopictus* is a vector of dengue and chikungunya across the world [6]. They breed in domestic environment, its preferred habitat are water storage tanks and jars inside and outside houses, tree holes, leaf axils, coconut shells, bottles and plant pots. They bite mainly in the mornings or evenings.

1.1.1.3 Mansonia

There are around 25 species of *Mansonia* (Figure 3(c)) which are mostly found in marshy areas of tropical countries. *Mansonia uniformis* is a vector of lymphatic filariasis agents, such as *Brugia malayi* in India and Southeast Asia and *Wuchereria bancrofti* in Asia and New Guinea. They are found in water bodies containing permanent vegetation such as swamps, ponds, grassy ditches and irrigation canals.

1.1.1.4 Haemagogus

There are around 25 species of *Haemagogus* (Figure 3(d)) which are only found in Central and South America. Several species of the Haemagogus are the main vector of transmission of selvatic yellow fever.

1.1.1.5 Sabethes

There are 39 species of Sabethes mosquitoes (Figure 3(e)) which are divided into five subgenera, are distributed in the Neotropical region. *Sabethes chloropterus* has been involved in the transmission of selvatic yellow fever in monkeys, accidentally in man, as well as arboviruses.

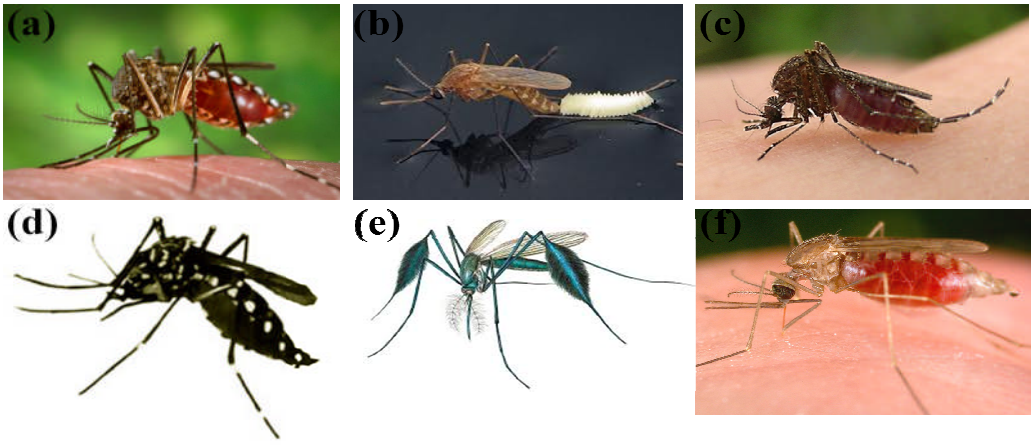

Figure 3: Different species of mosquito (a) *Aedes* (b) *Culex* (c) *Mansonia* (d) *Heamagogus* (e) *Seabthe* (f) *Anopheles*

1.1.2 Anophelinae

There are 484 described species of *Anopheles* (Figure 3(f)) principally known for their involvement as vectors of malaria pathogens. A number of *Anopheles* are also vectors of filariasis and viral diseases. They are distributed by geographical zone whereas some species of *Aedes* and *Culex* have a panmictic distribution. Their

behaviour can be anthropophilic/zoophilic, endophagic/exophagic or endophilic/exophilic.

1.1.3 Toxorhynchites

Toxorhynchites (Figure 4) are cosmopolitan genus (distributed all round the globe in appropriate habitat) of mosquitoes that are harmless to humans/do not suck blood. They are larger than other species and consume larvae of other mosquito species living in tree cervices. These species are introduced to areas outside their natural range in order to fight dengue fever.

Figure 4: *Toxorhynchites* mosquito

1.2 Repellents

Insect vectors especially mosquitoes are responsible for spreading human diseases such as malaria, Japanese encephalitis, yellow fever and filariasis as well as dengue. There is no foolproof vaccine to prevent the infection nor are the drugs to combat these diseases in infected persons so vector control is the most common solution for reducing morbidity. Apart from personal protections the repellent plays an important role in protection against arthropods because they can be used anywhere and anytime. Repellents are the substance which are resistant or impervious to other substances or species. They deter haematophagous arthropods and insects from sitting and biting on epidermal layer of human skin causing subcutaneous nodules thereby decreasing the disease transmission in many instances [7]. Rise in global warming enhances population growth of insects and arthropods in lower as well as higher altitudes. Insects living in warmer areas possess high metabolic rate and reproduce more which thereby increases the demand of repellents. The attraction of mosquitoes towards vertebrate host is largely mediated by the odour of the body emanations such as body heat, sweat (containing

lactic acid and 1-octene-3-ol in major quantity) and carbon dioxide [8]. CO_2 and 1-octene-3-ol emitted in human breath are the major attractant of the *Anopheles gambiae*. The mode of action of synthetic repellent like DEET has been reported via different mechanisms but the exact mechanism is not known till date. DEET blocks the olfactory receptor neurons (ORNs) sensitive to the lactic acid and strongly inhibits their electrophysiological activities. Evidence has revealed that the compounds containing the mixture of essential oils are also recognized by the receptor neurons but their mode of action is not well studied [9]. Repellents are broadly classified as natural and synthetic.

1.2.1 Synthetic Repellent

First synthetic repellent N, N-diethyl-m-toluamide (DEET), a broad spectrum repellent exhibited the best repellent properties with some pros and cons came into existence in 1956. Many other compounds have been characterized as having repellent activity for mosquitoes as well as other arthropod vectors based on laboratory behavioural bioassay or tropical application of the compounds to the skin for field and laboratory testing. Synthetic repellents that are commonly used in daily life are derivatives of amides (N, N-diethyl phenylacetamide (DEPA), ethyl N-acetyl-N-butyl-3-aminopropionate (IR3535), MGK 264, MGK 326); Diols (p-mentane-3,8-diol, ethyl hexane diol); piperidines (Picaridine, [sec-butyl2-(2-hydroxyethyl)piperidine-1-carboxylate (KBR 3023)) and phthalates (dioctyl phthalates, dimethyl carbate, dimethyl bicyclo[2.2.1]hept-2-ene-5,6 dicarboxylate (dimalone)). These repellents have been considered effective but adverse effects such as hypotension, decreased heart rate, anaphylaxis, urticaria syndrome and encephalopathy in children were observed. Risks associated with large quantity usage of chemical repellent led to the rise in several human health and environment related concerns. Repeated use of synthetic repellents has disrupted natural biological systems and often resulted in the development of resistance [4].

1.2.2 Natural/Botanical Repellent

Botanical repellents emerged as eco-friendly alternative which encompass microbial (bacteria, entomopathogenic fungi or viruses), pesticides, biochemical pesticides (pheromones) and plant incorporated protectants (genetically modified crops). Over 200 plants species contain chemicals with pest control properties; some of these

plants have repellent activity against mosquitoes [10]. Plants are an alternative source of mosquito repellents because they constitute a potential source of bioactive chemicals which are typically free from harmful effects. Generally most plants protect themselves from the attack of pytophagous insect by producing secondary metabolites known as allelochemicals or steroidal glycosides. These compounds mainly belong to the chemical category of nitrogen compounds, terpenoids, phenolics, proteinase inhibitors and growth regulators. Terpenoids, phenolics etc are effective against mosquitoes and haematophagous insects and hence considered as repellents. Plants like alder, basil, clove, marigold, spinach etc are widely used as herbal medicines in Europe, Japan and North America, thereby raising the confidence in their safety. Among all the plant families, promising essential oils from *Cymbopogon spp*. (citronella), *Ocimum spp.* (lemon) and *Eucalyptus spp.* (eucalyptus) act as essential ingredient in insect repellents which are applied on the skin. These natural products are frequently used due to their low toxicity, comparable efficacy and customer approval. Major component of EOs is terpenoids (monoterpenes); synthesized through biosynthetic pathways in the plant cells. 5-carbon dimethylallyl pyrophosphate (DMAPP) and its isomeric form isopentyl pyrophosphate (IPP) are the basic moieties required to obtain monoterpenes. These moieties are biosynthesized by methyl erythritol phosphate pathway in plastids. Both IPP and DMAPP condensed via geranyl pyrophosphate synthase to give the monoterpenes (Figure 5). The condensed product is further elongated by prenyltransferases to give farnesyl pyrophosphate (FPP), precursor of sesquiterpenes and geranyl geranyl pyrophosphate (GGPP), precursor of diterpenes. In plastid monoterpenes and diterpenes yield camphene, thujone and pinane ring like structures in the presence of different cyclases [11].

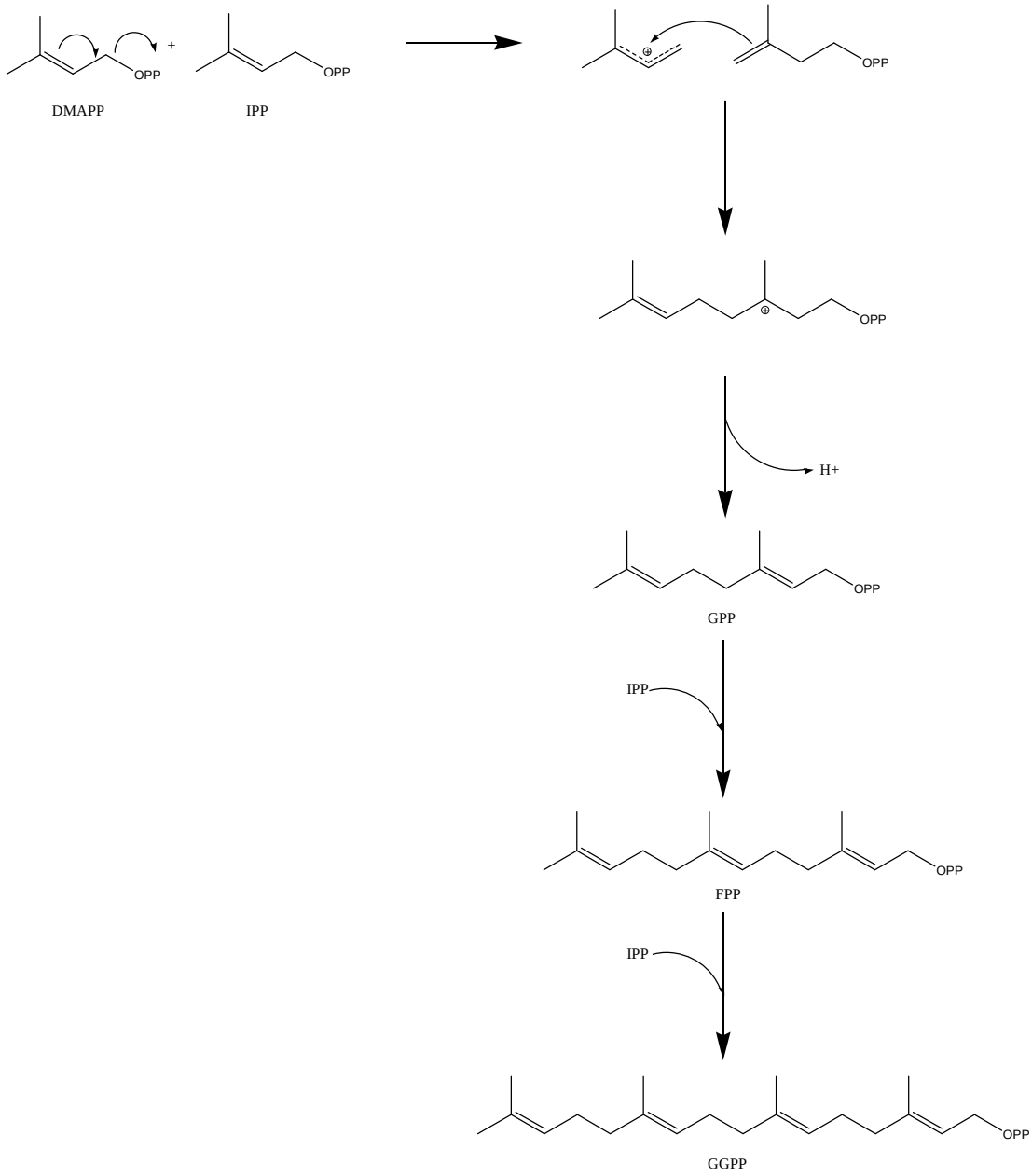

Figure 5: Biosynthetic pathway to form GPP, FPP and GGPP in plastids [11]

Monoterpenes present in EOs may contain terpenes that are hydrocarbons (α-pinene), alcohols (menthol, geran- iol, linalool, terpinen-4-ol, p-menthane-3,8-diol), aldehydes (cinnamaldehyde, cuminaldehyde), ketones (thujone), ethers [1,8-cineole (eucalyptol)], and lactones (nepetalactone) [12] (Figure 6) while among sesquiterpenes, β-caryophyllene is the most efficient repellent. However, the combination of monoterpenoids and sesquiterpenoids has emerged out to be the highly effective repelling system.

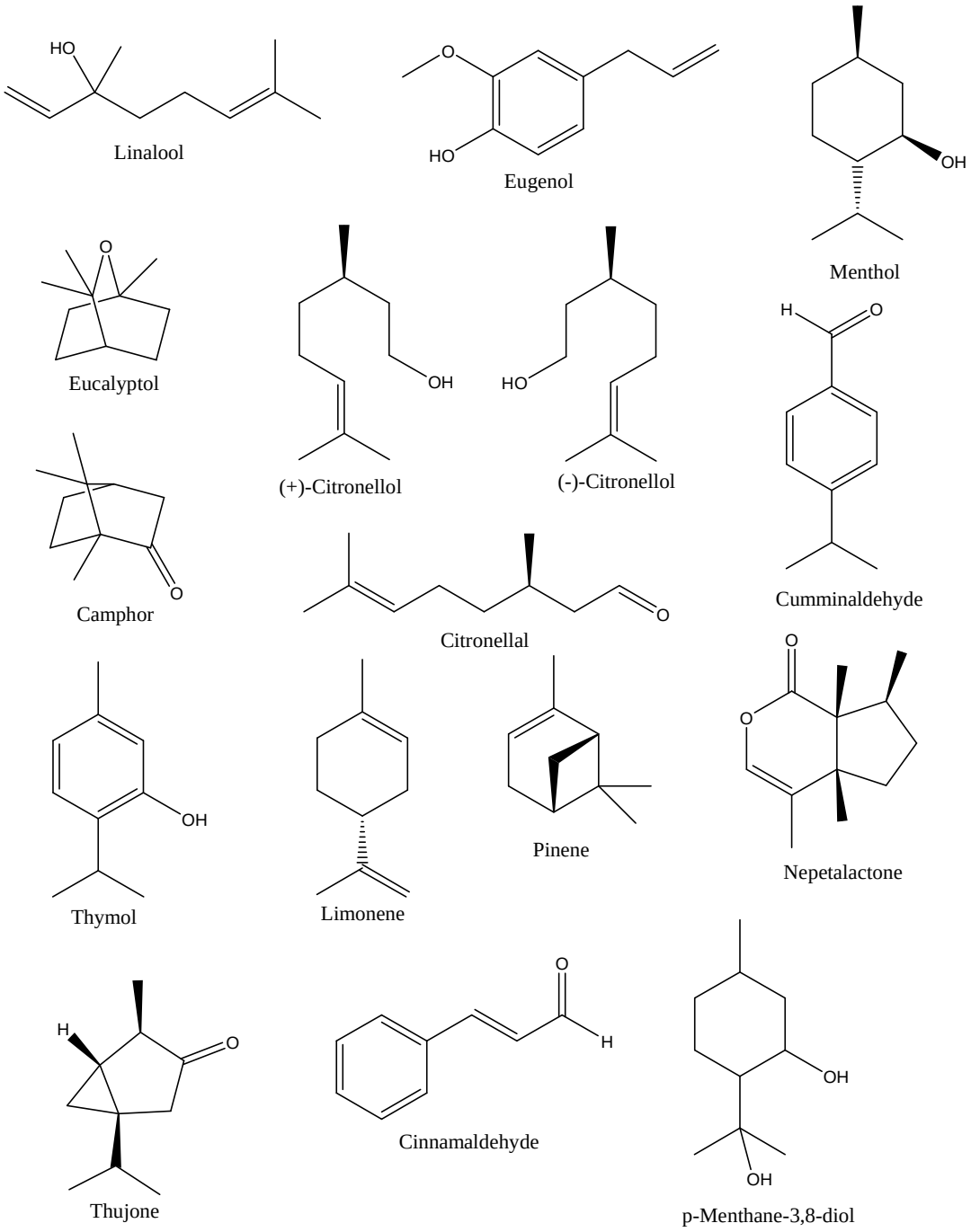

Figure 6: Representative constituents of Essential Oils

1.3 Aim of the thesis

In this study we focus on the development of novel mosquito repellents both botanically as well as synthetically. Botanical repellent has been isolated from the *Lantana camara* plant belonging to Verbenaceae family. *Lantana camara* essential oil was extracted from the leaves of the plant by Clevenger distillation apparatus (Figure 7). The oil was characterized by GC-MS technique to know the different

constituents/metabolites present in oil. *Lantana* oil is also an effective antibacterial agent hence the antibacterial property of the oil was examined by incorporating oil in polyacrylonitrile (PAN) matrix and making a composite membrane. Stability of the oil in PAN was accessed by XiGo nano tool while the surface morphology was examined by AFM and FESEM. Antibacterial activity was checked by disk diffusion method against gram positive and gram negative stains. Diffusion of the oil from the membrane was studied through molecular simulation by using Material Studio software. Mosquito repellency was accessed by hand in cage method as per the WHO standards [13].

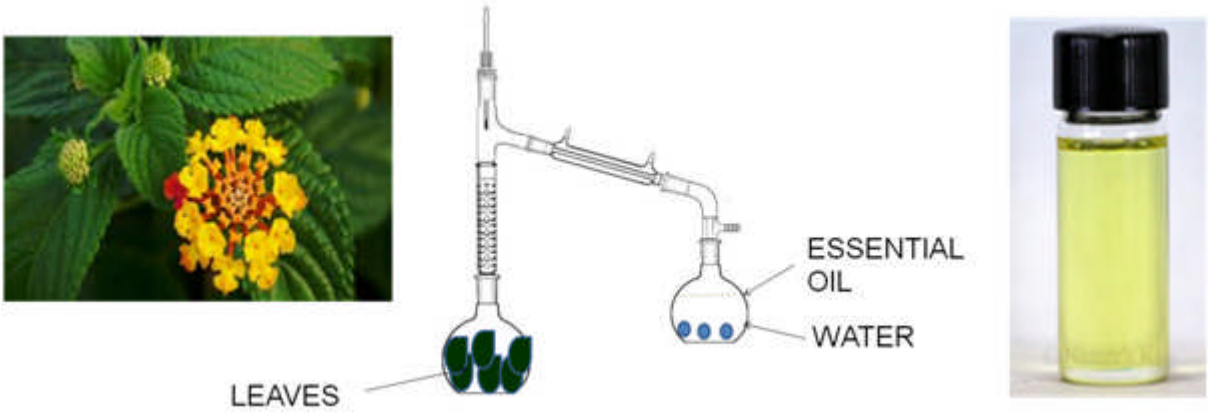

Figure 7: Extraction of oil using Clevenger distillation apparatus

Nitrogen containing compounds (amides and imides) are considered to possess long duration protection against arthropods as compared to the alcohols, esters and lactones, ethers and acetals [14]. Ellin et. al. identified 130 compounds found in total human body emanations among which maximum effects the host seeking behaviour of mosquitoes [15]. Pyruvic acid, an oxo acid obtained through glycolysis of glucose plays a vital role in human metabolism under aerobic conditions is also one of the body emanation. With this background we have synthesized some repellents similar to DEET (N, N diethyl-3-methylbenzamide) but with greater efficacy and negligible side effects through simple chemical routes. Pyruvic acid was coupled with substituted benzamide constituents, combination of both the moieties results in an efficient synthetic repellent. Repellents were characterized by NMR, FTIR, HR-MS and the mosquito repellency was tested by hand in cage experiment as per the WHO standard [13].

Materials and Methods

2.1 Materials

Polyacrylonitrile ($\overline{M_w}$: 150,000), Dimethyl sulfoxide (DMSO), Dimethylformamide (DMF), anhydrous sodium sulphate, 3-Methyl-4-nitrobenzoic acid, diethyl amine, diisopropyl amine, dibutyl amine, dihexyl amine, pyruvic acid, Thionyl chloride ($SOCl_2$), Fe powder were purchased from Sigma Aldrich, India and Phosphate buffer solution (PBS) (pH= 7.4) from Thomas Baker. DMEM (Dulbecco's Modified Eagle Medium) containing 10% fetal bovine serum (FBS) was purchase from Gibco, India. Bacterial strains; Gram-negative (*Escherichia coli* MTCC-1650) and Gram-positive (*Bacillus subtilis* MTCC-441) were used for antibacterial evaluations. The mouse embryonic fibroblasts cell line (NIH 3T3) was obtained from National Centre for Cell Science (NCCS), Pune were used for cell viability test.

2.2 General Reaction Procedures

2.2.1 Synthesis of N,N-Dialkyl-3-methyl-4-nitro benzamide (DAB):

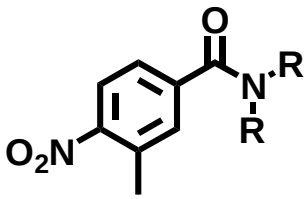

Thionyl chloride (0.875 mL. 1.4 g, 12.14 mmol) was added to a stirred solution of 3-methyl-4-nitro benzoic acid (2 g, 11.04 mmol) in 50 mL of toluene containing a drop of N,N-dimethylformamide at reflux, and the resulting solution was stirred for 2 h at reflux under nitrogen atmosphere. The reaction mixture was concentrated and the residue was dissolved in 30 mL of diethyl ether. Dialkyl amine (12.14 mmol) in 10 mL diethyl ether was added drop-wise, and the resulting mixture was for 1 h at ambient temperature under nitrogen atmosphere. The reaction mixture was poured into water, and the product was extracted in diethyl ether. The combined ether extract was washed with 10% HCl, saturated $NaHCO_3$ and bride, dried over Na_2SO_4 and concentrated. The crude product was purified via chromatography on SiO2 eluted with ether and was then recrystallized from MeOH to give 1.9 g of amide as a light yellow crystalline solid N,N-Dialkyl-3-methyl-4-nitro benzamide, yield %= 73% [16].

2.2.2 Synthesis of 4-Amino- N,N-dialkyl -3-methyl-benzamide (ADB):

Iron powder (2.12 g, 37.8 mmol, 10 equiv.) and concd. hydrochloric acid (ca. 50 mg) were added to the stirred solution of N,N-Dialkyl-3-methyl-4-nitro benzamide (3.7

mmol) in EtOH (30 mL) and water (7.5 mL), and the mixture was heated to reflux for 90 min under nitrogen atmosphere.

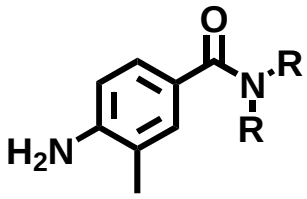

EtOAc (150 mL) was added to the mixture and then filtered. Filterate was washed 5-6 times with distilled water to remove the reddish colour of the filterate. EtOAc fraction was dried with Na_2SO_4 and then concentrated under reduced pressure. The crude product was purified by chromatography on SiO_2, PE/EA=7:1 to give 0.640 g of 4-Amino-N,N-dialkyl-3-methyl benzamide as a orange liquid. Yield %=72.23 % [17]

2.2.3 Synthesis of N,N-dialkyl-3-methyl-4-(3-oxo-propionylamino)-benzamide (Pyr-ADB):

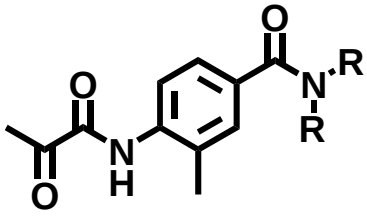

Thionyl chloride (0.185 mL. 0.297 g, 2.5 mmol) was added to a stirred solution of Pyruvic acid (0.2 g, 2.27 mmol) in 30 mL of toluene containing a drop of N,N-dimethylformamide at reflux, and the resulting solution was stirred for 2 h at reflux under nitrogen atmosphere. The reaction mixture was concentrated and the residue was dissolved in 30 mL of diethyl ether. 4-Amino- N,N-dialkyl -3-methyl-benzamide (2.5 mmol) in 10 mL diethyl ether was added drop-wise, and the resulting mixture was for 1 h at ambient temperature under nitrogen atmosphere. The reaction mixture was poured into water, and the product was extracted in diethyl ether. The combined ether extract was washed with 10% HCl, saturated $NaHCO_3$ and bride, dried over Na_2SO_4 and concentrated. The crude product was purified via chromatography on SiO2 eluted with ether to give 0.210 g of reddish liquid of N,N-dialkyl-3-methyl-4-(3-oxo-propionylamino)-benzamide, yield %= 27%

2.3 Characterization Method

NMR was recorded in a 400 MHz Jeol NMR spectrometer in $CDCl_3$ containing a small amount of TMS as internal standard. 10 mg of compound was dissolved in 0.75 mL $CDCl_3$ and was filled in NMR tube. FT-IR spectra of all compounds were recorded on a Thermo Scientific Nicolet 6700 FTIR spectrometer using potassium bromide (KBr) pellet prepared from powdered sample (3 mg) mixed with dry KBr. The spectra were recorded in the absorbance mode from 4000 to 400 cm^{-1}. Mass of all the synthesized compounds was confirmed using the Applied Biosystems 4800 PLUS MALDI TOF/TOF analyzer.

2.4 Extraction and characterization of *Lantana camara* oil

Shade dried leaves (1 Kg) of *Lantana camara* were subjected to hydro-distillation in a conventional Clevenger type apparatus for 10 hr to extract the essential oil. Light yellow colour oil (0.92 g, <1% yield) obtained by decantation was dried over anhydrous sodium sulphate and stored at 4 ˚C. Essential oil composition was determined using Shimadzu GC–2010 coupled with Perkin-Elmer Turbo Mass spectrometer using a PE-Wax (30 m × 0.32 mm i.d., film thickness 0.25 µm) column. Oven temperature initially kept 70 ˚C was raised to 120 ˚C at 2 ˚C/min and then raised to 240 ˚C at 3 ˚C/min; injector temperature was maintained at 250 ˚C and helium acted as carrier gas for the molecular ions. EO constituents were analyzed by mass spectrometer (ion trap at 220 ˚C; manifold at 80 ˚C and transfer line at 240 ˚C). The MS fragmentation pattern was checked by matching with NIST mass spectra libraries.

2.5 Preparation of composite membrane

Lantana camara-PAN composite and Pyr-ADB derivative composite membranes were prepared by solvent casting technique. Briefly 5 wt% of PAN and 10 mL DMSO were initially charged in 100 mL beaker. After the PAN fully dissolved, 0.02 % (v/v) of *Lantana* Oil and 0.25 µg of Pyr-ADB derivatives were added. The solution was vigorously stirred for 30 min at room temperature and then kept under vacuum for 30 min for degassing. This mixture was casted on a glass petri and dried at room temperature to obtain thin membrane. The obtained membrane was washed with deionised water and dried in ambient atmosphere for 12 hr and stored in vacuum [18].

2.6 Stability of the oil in PAN matrix

Solvent relaxation NMR experiments were performed to assess the stability of *Lantana* oil in the homogeneous solution of PAN through interfacial solvent displacement using the Acron Area particle sizer from XiGo Nanotools. The Carr-Purcell-Meiboom-Gill (CPMG) pulse sequence was used with a spacing between the 180° pulses of 1 ms (i.e.,τ = 0.5 ms), averaging 4 scans with a recycle delay of 2480 ms. Spin-spin relaxation rates (T2) were obtained by fitting a single exponential to the phase and baseline corrected signal. The stability of the particles in the solution attributed to the homogeneous dispersion of oil droplets i.e. droplets do not aggregate or settle at the stipulated time period. These measurements were carried out in NMR tubes having outer diameter 5 mm. 0.5 mL samples were placed in different NMR tubes such that the tubes are filled till the minimum height of 54 mm ensuring that no air bubbles are trapped. The tubes were capped to prevent drying of samples. For accurate results, the tubes were filled to the same volume. Initially, the bulk relaxation time (T1) of pure solvent (DMSO) expressed in ms was quantified and saved as reference value for determining the relaxation time (T2) for polymer composite [19].

2.7 Morphology of composite membrane

Surface topology of the resulting membrane was investigated via atomic force microscopy (AFM, Asylum Research) in contact mode using silicon tip with a cantilever, with constant force and resonant frequency of 13 kHz and 0.2 N/m respectively and at 256 points/line and 1 points/line. PAN membrane surfaces were imaged in a scan size of 10*10 μm. Images were captured at different locations and the roughness factor was calculated using the WSxM 5.0 Developer 6.4 software. The morphology of the sample was observed using FE-SEM (JSM-6700F, JEOL, Japan). The membrane was mounted on aluminium stubs using double sided carbon conducting tape [20]. Contact angle measurement was performed by drop shape analysis system (KRUSS DSA25). 8 µL of phosphate buffer solution droplet was used for the contact angle measurement.

2.8 *In-vitro* antibacterial assay

The nutrient agar medium in petri dish was inoculated with 0.1 mL, 10^7-10^8 cfu/mL freshly grown *B. subtilis* or *E. coli.* The prepared membranes were cut into 6 mm

diameter disk using a hole-puncher and were kept on the microbial cultures. Bacterial stains were incubated at 37±2 ˚C and 50±2% reltive humidity for 24 hours. After incubation the results were visually assessed by inhibition zone which is measured by vernier caliper and the photographs were taken [18].

2.9 *In-vitro* release study

Theoretical release study of oil from the membrane was monitored using UV–Vis spectrometer (Ocean Optics, HR4000). 0.1 g of composite membrane was immersed in 10 mL phosphate buffer solution (PBS, pH = 7.4) used as release medium. The aliquot from the release medium was periodically collected and added to 1 mL DMSO, the solution is mixed well and the UV-Vis Spectrum was noted [21].

2.10 Characterization of cytotoxicity

Viability of the cells was determined by yellow water soluble tetrazolium salt,3-[4,5-dimethylthiazol-2-yl]2,5-diphenyltetrazolium bromide (MTT). The monolayer cells were detached with trypsin-ethylenediaminetetraacetic acid (EDTA) to make single cell suspensions and viable cells were counted using a hemocytometer and diluted with medium containing 5% FBS to give final density of $1x10^5$ cells/mL. One hundred microlitres per well of cell suspension were seeded into 96-well plates at plating density of 10,000 cells/well and incubated at 37 ˚C to allow cell attachment. After 24 h the cells were treated with serial concentrations of the test samples which were dissolved in dimethylsulfoxide (DMSO). The plates were further incubated for an additional 48 h at 37 ˚C upon addition of sample. The medium containing without samples were served as control and triplicate was maintained for all concentrations. After 48 h of incubation, 15 µL of MTT (5mg/ml) in phosphate buffered saline (PBS) was added to each well and incubated at 37 ˚C for 4 h. Absorbance of fromazan crystal dissolved in 100 µL DMSO at 570 nm was measured using micro plate reader.The percentage cell viability was then calculated with respect to control using Eq (1) [22].

$$\% \text{ Cell viability} = [A] \text{ Test} / [A]\text{control} \times 100 \quad (1)$$

2.11 Details of Simulation

Molecular dynamics simulations were carried out using the Amorphous Cell and Forcite module of Material Studio, which was developed by Accelrys Software Inc.

The COMPASS (condensed phase optimization molecular potentials for atomistic simulation studies module) developed by Sun [23] was used in the study. Geometry optimization and the interaction energies of the E-cryophyllene and the polymer, mean square displacement of polymeric chain, diffusion coefficient and free volume calculation have been performed. The molecular dynamic simulation was performed in the NVT ensemble for calculating the diffusion coefficient.

2.12 Mosquito Repellence Test

Mosquito repellence activity was assessed on the basis of protection period (hr) offered by various analogues of synthetic and natural repellents against mosquito bites [24]. The protection period was measured on the basis of the concept "time until the first bite" pioneered by Garnette. Repellence tests were carried out against 3-5 days old, blood starved but sucrose fed (0.5 M solution), *Aedes aegypti* mosquitoes, drawn from well established laboratory colony maintained at 27±1 ˚C temperature and 70±5 % relative humidity. The light intensity was regulated at 300-500 lux for testing against laboratory, colonized *Aedes aegypti* (day biting mosquito). Human volunteer's hand covered with polythene disposable gloved introduced in the cage containing about 200 hungry mosquitoes. Mosquitoes were allowed to bite on the back of the hand trough muslin screen stuck over a small window (2 cm x 2 cm) cut in the polythene bag. Various analogues of synthetic and natural repellents were loaded on the muslin cloth screen instead of direct skin application so as to avoid the potential risk involved in the evaluation of natural and synthetic products of unknown mammalian toxicity. All the test solutions were made in analar grade acetone. Muslin cloth screen was treated with the analogues taking doses of 0.25 mg/cm^2, 0.5 mg/cm^2, 0.75 mg/cm^2, 1.5 mg/cm^2 and the solvent was evaporated before use. Control muslin screen was treated with solvent alone. After introduction of the hand covered with the polythene glove with the treated muslin screen into the mosquito cage, numbers of mosquito bites received in subsequent 5 minutes were counted. In the event of number of bites in the initial 5 minutes exposure, the test hand was exposed repeatedly after every consecutive 30 minutes for 5 minutes till the time a confirmed bite was received. Number of hours before the receipt of a confirmed bite [25] represented the protection period offered by the test compound. In control rate of mosquito bite was 10-12 bites/min. Above tests were repeated with both male and female human volunteers using different mosquito batches. N, N-diethyl-m-toluamide

(DEET) was used as positive control. All the tests were carried out at 27±1 ˚C temperature between 9:00 – 17:00 hrs.

RESULTS AND DISSCUSSION

3.1 Synthesis of Pyr-ADB derivatives and their characterization

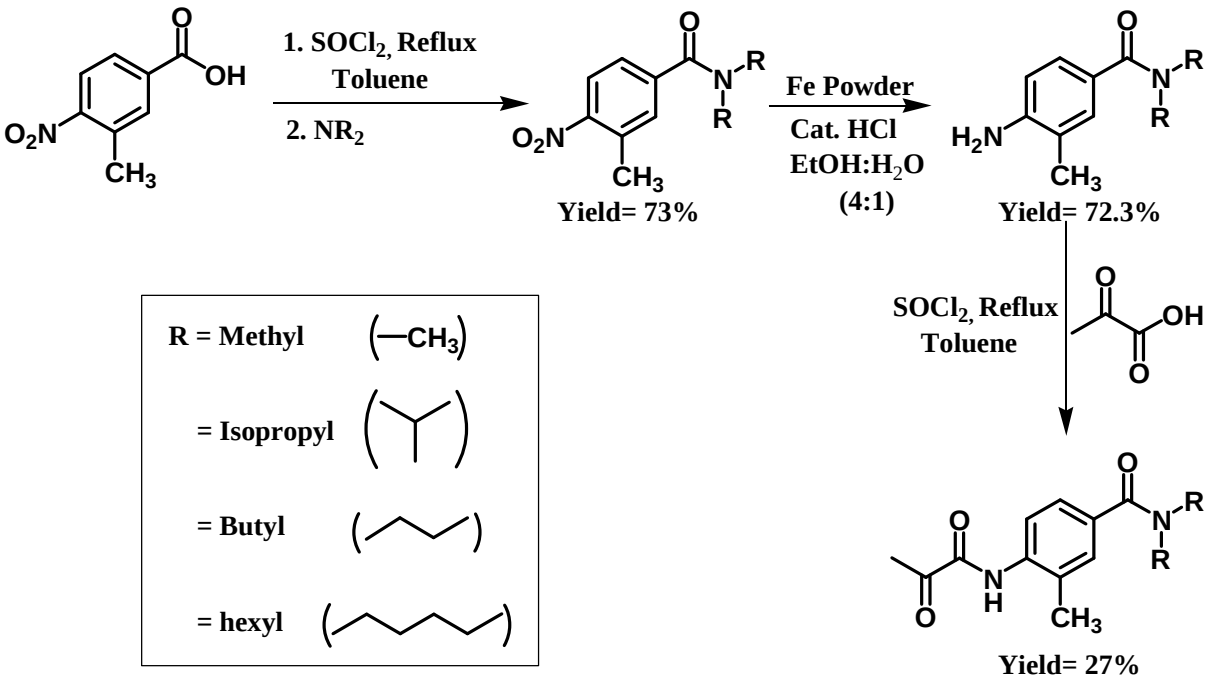

Scheme 1: Synthesis of Pyr-ADB-dialkyl

3.1.1 Synthesis of Pyr-ADB-Diethyl (PE)

Pyruvic acid, an oxo acid obtained through glycolysis of glucose plays a vital role in human metabolism under aerobic conditions is also one of the body emanation was grafted to a synthsized diethyl substituted benzamide constitutent using SN_2 mechanism followed by amidation (see scheme 1). Briefly, 3-methyl-4-nitrobenzoic acid was reacted with diethyl amine in presence of $SOCl_2$ to give DAB-diethyl. Nitro group of DAB-diethyl was reduced to amine in the presence of iron powder and cat. HCl to give ADB-diethyl which was further coupled to pyruvic acid to give Pyr-ADB-diethyl. ^{1}H spectrum of DAB-diethyl was recorded in CDCl3 showed peaks from 7.3-8.01 ppm corresponding to aryl protons while peak at 3.2 and 3.54 ppm was designated to N-**CH_2**, peak at 2.62 ppm corresponds to Ar-**CH_3** and peak at 1.11 and 1.25 ppm corresponds to N-(CH_2-**CH_3**)$_2$. Upon conversion to ADB-diethyl peak of **NH_2** merges with N-**CH_2** resulting in a broad peak at 3.4 ppm. Upon coupling with Pyruvic acid addition peak of COCO**CH_3** appears at 2.15 ppm. ^{1}H NMR (400 MHz, $CDCl_3$) δ: 8.21 (s, 1H, Ar-**H**), 7.25 (m, 2H, Ar-**H**), 2.57 (s, 3H, Ar-**C**H_3), 3.31 and 3.48 (q, 2H, N-(**C**H_2CH_3)$_2$), 2.29 (s, 3H, COCO-**CH_3**), 1.23 (t, 6H, N-(CH_2**C**H_3)$_2$). ^{13}C NMR (100 MHz, $CDCl_3$) δ: 197.4 (CH_3-**C**O), 170.5 (Ar-**C**O), 157.6 (CH_3-CO**C**O), 136.0, 134.8, 128.4, 124.3, 120.9 (Ar-**C**), 29.8 (N-**C**H_2CH_3), 24.2 (**C**H_3-CO), 20.9 (CH_2**C**H_3),

17.5 (Ar-**C**H_3). FT-IR ((KBr), cm^{-1}): 3450 (N-H stretch), 3240 (Aromatic C-H stretch), 2930, 2870 (Aliphatic C-H stretch), 1770 (C=O stretch), 1720, 1610, (amide C=O stretch), (MW: 276.33), m/z= 315.16 ($M+K^+$)

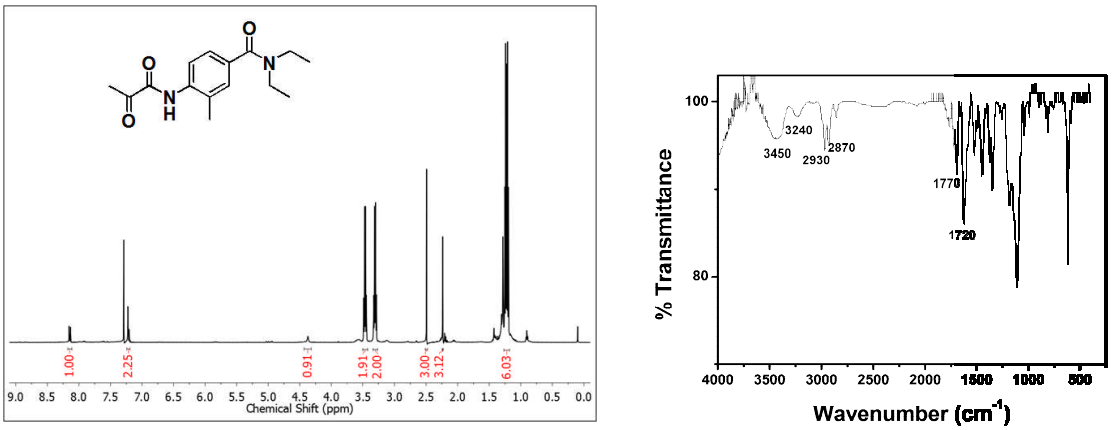

Figure 8: NMR and FT-IR spectra of Pyr-ADB-diethyl

3.1.2 Synthesis of Pyr-ADB-diisopropyl (PI)

Briefly, 3-methyl-4-nitrobenzoic acid was reacted with diethyl amine in presence of $SOCl_2$ to give DAB-diisopropyl. Nitro group of DAB-diisopropyl was reduced to amine in the presence of iron powder and cat. HCl to give ADB-diisopropyl which was further coupled to pyruvic acid to give Pyr-ADB-diisopropyl. ^{1}H spectrum of DAB-diisopropyl was recorded in $CDCl_3$ showed peaks from 7.25-7.99 ppm corresponding to aryl protons while peak at 3.7 and 3.53 ppm was designated to N-**CH_2**, peak at 2.60 ppm corresponds to Ar-**CH_3** and peak at 1.53 and 1.15 ppm corresponds to N-(CH_2-**CH_3CH_3**)$_2$. Upon conversion to ADB-diethyl peak of **NH_2** merges with N-**CH_2** resulting in a broad peak at 3.75 ppm. Upon coupling with Pyruvic acid addition peak of COCO**CH_3** appears at 2.13 ppm. ^{1}H NMR (400 MHz, $CDCl_3$) δ: 8.14 (m, 2H, Ar-**H**), 6.26 (s, 1H, Ar-**H**), 3.82 and 3.48 (m, 1H, N-(**CH_2**CH_3)$_2$)), 2.39 (s, 3H, Ar-**CH_3**), 2.01 (s, 3H, COCO-**CH_3**), 1.52 and 1.25 (d, 12H, N-(CH**CH_3** **CH_3**)$_2$). ^{13}C NMR (100 MHz, $CDCl_3$) δ: 197.4 (CH_3-**C**O), 170.5 (Ar-**C**O), 157.6 (CH_3-CO**C**O), 136.0, 134.8, 128.4, 124.3, 120.8 (Ar-**C**), 29.7 (N-**C**H_2CH_3), 24.2 (**C**H_3-CO), 20.9 (CH_2**C**H_3), 17.5 (Ar-**C**H_3). FT-IR ((KBr), cm^{-1}): 3380 (N-H stretch), 3340 (Aromatic C-H stretch), 2970, 2860 (Aliphatic C-H stretch), 1780 (C=O stretch), 1700, 1620, (amide C=O stretch), (MW: 304.38), m/z= 343.24 ($M+K^+$).

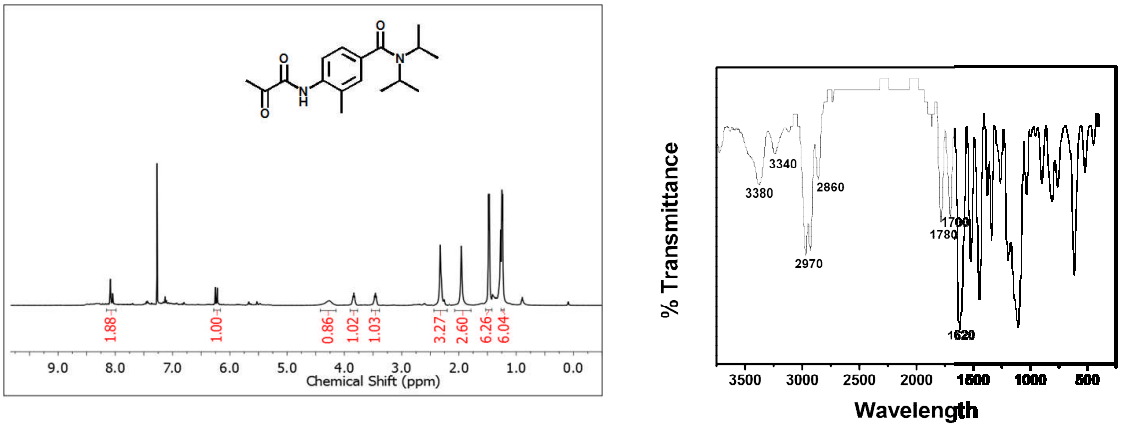

Figure 9: NMR and FT-IR spectra of Pyr-ADB-diisopropyl

3.1.3 Synthesis of Pyr-ADB-dibutyl (PB)

Briefly, 3-methyl-4-nitrobenzoic acid was reacted with diethyl amine in presence of $SOCl_2$ to give DAB-dibutyl. Nitro group of DAB-dibutyl was reduced to amine in the presence of iron powder and cat. HCl to give ADB-dibutyl which was further coupled to pyruvic acid to give Pyr-ADB-dibutyl. ^{1}H spectrum of DAB-dibutyl was recorded in $CDCl_3$ showed peaks from 7.25-7.99 ppm corresponding to aryl protons while peak at 3.46 and 3.12 ppm was designated to N-$\mathbf{CH_2}$, peak at 2.60 ppm corresponds to Ar-$\mathbf{CH_3}$, peak at 1.62 and 1.47 ppm corresponds to N-(CH_2-$\mathbf{CH_2}$-CH_2-CH_3)$_2$, peak at 1.37 and 1.12 ppm corresponds to N-(CH_2-CH_2-$\mathbf{CH_2}$-CH_3)$_2$ and peak at 0.96 and 0.79 ppm corresponds to N-(CH_2-CH_2-CH_2-$\mathbf{CH_3}$)$_2$. Upon conversion to ADB-diethyl peak of $\mathbf{NH_2}$ merges with N-$\mathbf{CH_2}$ resulting in a broad peak at 3.75 ppm while other doublet of doublet peak merges to give single broad peak. Upon coupling with Pyruvic acid addition peak of COCO$\mathbf{CH_3}$ appears at 2.13 ppm. ^{1}H NMR (400 MHz, $CDCl_3$) δ: 7.25 (s, 1H, Ar-**H**), 6.85 (m, 2H, Ar-**H**), 4.34 (b, 1H, **NH**), 3.47 and 3.23 (t, 2H, N-($\mathbf{CH_2}CH_2CH_2CH_3$)$_2$), 2.48 (s, 3H, Ar-$\mathbf{CH_3}$), 2.0 (s, 3H, COCO-$\mathbf{CH_3}$), 1.32 (m, 8H, N-($CH_2\mathbf{CH_2CH_2}CH_3$)$_2$), 0.98 (t, 6H, N-($CH_2CH_2CH_2\mathbf{CH_3}$)$_2$). ^{13}C NMR (100 MHz, $CDCl_3$) δ: 197.4 (CH_3-**C**O), 172.3 (Ar-**C**O), 145.8 (CH_3-CO**C**O), 131.0, 129.5, 127.0, 126.0, 121.7, 114.0 (Ar-**C**), 30.9 (N-**C**H_2CH_3), 29.8 (**C**H_3-CO), 20.1 (CH_2**C**H_3), 17.4 (Ar-**C**H_3). FT-IR ((KBr), cm^{-1}): 3450 (N-H stretch), 3240 (Aromatic C-H stretch), 2930, 2870 (Aliphatic C-H stretch), 1770 (C=O stretch), 1720, 1620, (amide C=O stretch), (MW: 332.44), m/z= 371.21 ($M+K^+$)

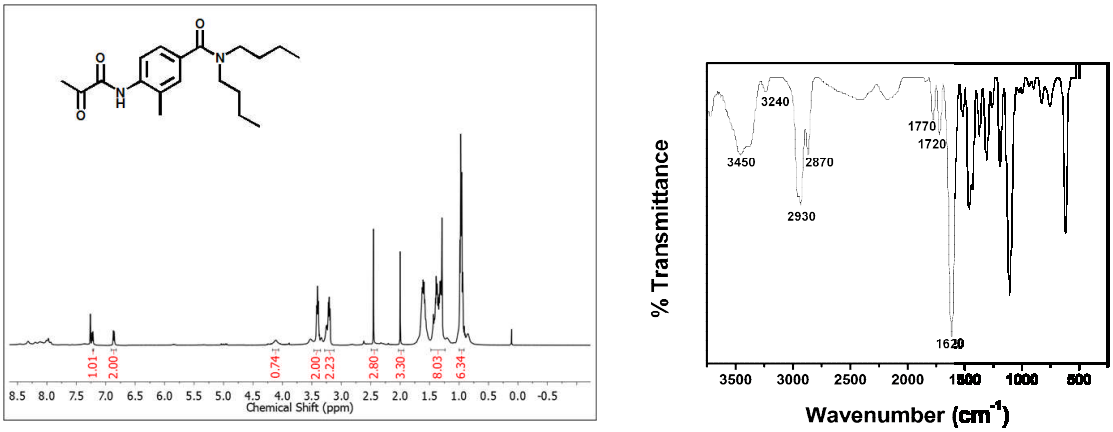

Figure 10: NMR and FT-IR spectra of Pyr-ADB-dibutyl

3.1.4 Synthesis of Pyr-ADB-dihexyl (PH)

Briefly, 3-methyl-4-nitrobenzoic acid was reacted with diethyl amine in presence of $SOCl_2$ to give DAB-dihexyl. Nitro group of DAB-dihexyl was reduced to amine in the presence of iron powder and cat. HCl to give ADB-dihexyl which was further coupled to pyruvic acid to give Pyr-ADB-dihexyl. ^{1}H spectrum of DAB-dihexyl was recorded in $CDCl_3$ showed peaks from 7.25-7.99 ppm corresponding to aryl protons while peak at 3.45 and 3.11 ppm was designated to N-**CH_2**, peak at 2.60 ppm corresponds to Ar-**CH_3**, peak at 1.63 and 1.49 ppm corresponds to N-(CH_2-**CH_2**-CH_2-CH_2-CH_2-CH_3)$_2$, peak at 1.33 ppm corresponds to N-(CH_2-CH_2-**CH_2**-CH_2-CH_2-CH_3)$_2$, peak at 1.19 and 1.10 ppm corresponds to N-(CH_2-CH_2-CH_2-CH_2-**CH_2**-CH_3)$_2$ and peak at 0.89 and 0.81 ppm corresponds to N-(CH_2-CH_2-CH_2-CH_2-CH_2-**CH_3**)$_2$. Upon conversion to ADB-diethyl peak of **NH_2** merges with N-**CH_2** resulting in a broad peak at 3.75 ppm while other doublet of doublet peak also merges to give single broad peak. Upon coupling with Pyruvic acid addition peak of COCO**CH_3** appears at 2.10 ppm. ^{1}H NMR (400 MHz, $CDCl_3$) δ: 7.07 (s, 1H, Ar-**H**), 6.64 (m, 2H, Ar-**H**), 4.29 (b, 1H, **NH**), 3.30 (b, 2H, N-(**CH_2**$CH_2CH_2CH_2CH_2CH_3$)$_2$), 2.14 (s, 3H, Ar-**CH_3**), 2.02 (s, 3H, COCO-**CH_3**), 1.53 (b, 2H, N-(CH_2**CH_2**$CH_2CH_2CH_2CH_3$)$_2$), 1.22 (b, 6H, N-(CH_2CH_2**$CH_2CH_2CH_2$**CH_3)$_2$), 0.84 (b, 6H, N-($CH_2CH_2CH_2CH_2CH_2$**CH_3**)$_2$). ^{13}C NMR (100 MHz, $CDCl_3$) δ: 198.4 (CH_3-**C**O), 172.3 (Ar-**C**O), 144.0 (CH_3-CO**C**O), 131.0, 129.5, 127.0, 126.0, 121.7, 114.0 (Ar-**C**), 30.9 (N-**C**H_2CH_3), 29.8 (**C**H_3-CO), 23.1, 22.0, 21.8, 20.6 (Aliphatic-**C**), 17.4 (Ar-**C**H_3). FT-IR ((KBr), cm^{-1}): 3380 (N-H stretch), 3240 (Aromatic C-H stretch), 2930, 2890 (Aliphatic C-H stretch), 1700, 1620, (amide C=O stretch), (MW: 388.54), m/z= 427.27 ($M+K^+$)

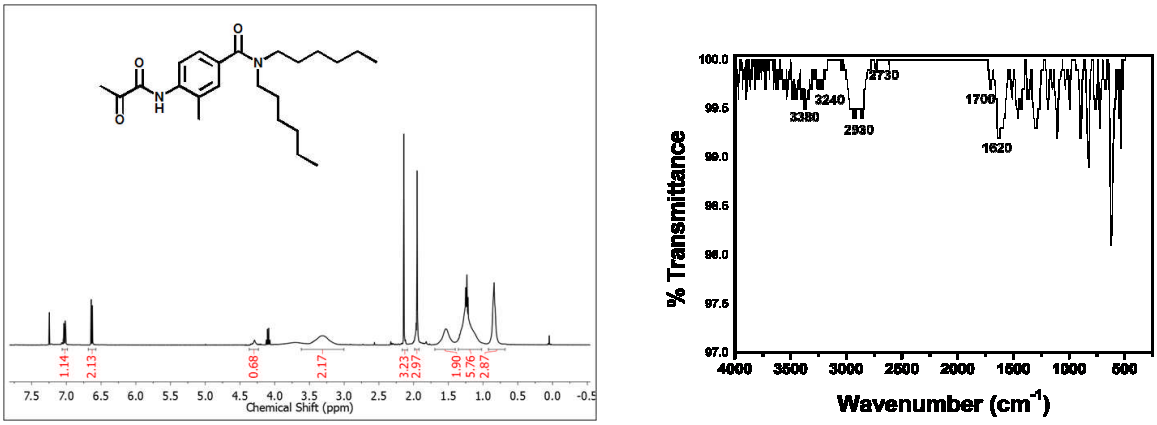

Figure 11: NMR and FT-IR of Pyr-ADB-dihexyl

3.2 Characterization of oil

The maximum yield of oil extracted from the *Lantana Camara* leaves was 0.92%. The GC profile of the oil (Figure 12) is highly compatible with the literature reports [26]. The components of the oil were identified by comparison of the mass spectra with those from the NIST computer library and with authentic compounds published in the literature. E-Caryophyllene (19.7%) with retention time of 3.7 min is major anti-bacterial agent present in the oil. Other major compounds identified were germacrene D, α-humulene, sabinene and caryophyllenoxide.

$$Yield\ \% = \frac{Amount\ of\ oil\ obtailed\ (\ in\ grams)}{Amount\ of\ leaves\ taken\ (\ in\ grams)} * 100$$

$$Yield\ \% = \frac{9.2\ g}{1000\ g} * 100$$

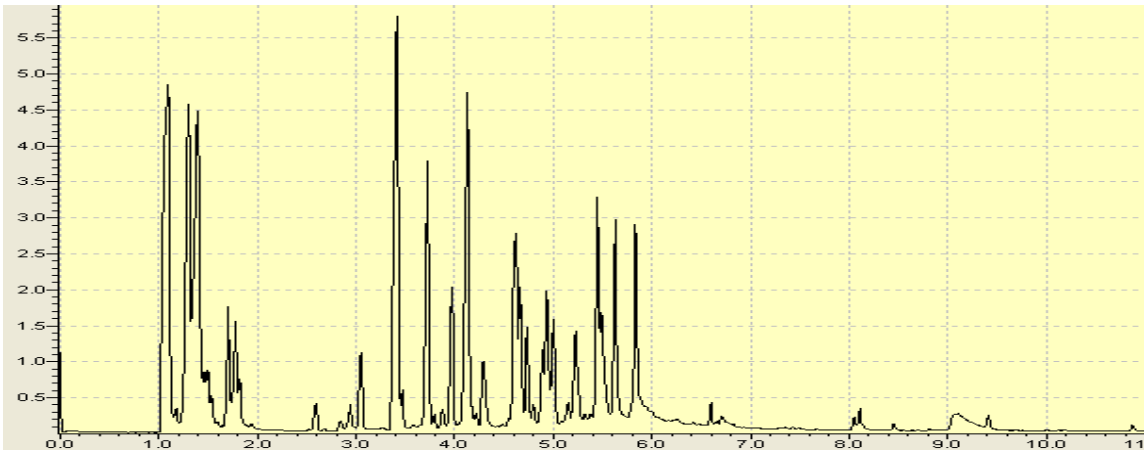

Figure 12: GC profile of *Lantana* oil

3.3 Stability of oil in PAN matrix

0.02 wt% oil formed a stable composite membrane with 5% PAN as compared to the 0.01 wt% and 0.03 wt%. 0.01 % (v/v) of oil in 5 wt% PAN membrane formed a stable membrane but since the concentration of PAN is very high the amount of oil oozing out from the membrane is almost equivalent to negligible hence no zone of inhibition could be observed for the anti bacterial assay. While 0.03 % (v/v) oil in 5 wt% PAN lead to the uneasiness in handling of the membrane. Membrane formed was very fragile as it was releasing large amount of water hence it was creating hindrance in morphometric studies. Stability of oil in PAN matrix was monitored using surface area analyzer, which revealed high stability of the system without any agglomeration (Figure 13). The composite system exhibited constant relaxation time of 1487 time/sec with 306 echo cycles and 4 averaging scans for 3000 sec which corresponds to high stability of the system [17].

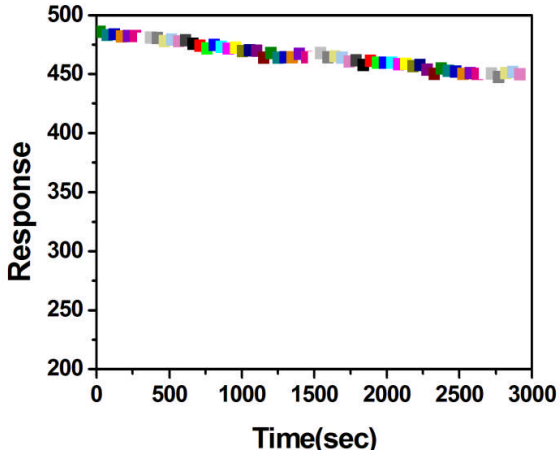

Figure 13: Stability profile of the oil in PAN matrix

3.4 Membrane morphology

Surface topology of the composite membrane as investigated from AFM (Figure 14(a)) indicated roughness factor of 0.9 nm which corresponds to highly hydrophilic surface because the degree of roughness is directly proportional to the hydrophilicity [27]. Decreased surface roughness also corresponds to minimum agglomeration of oil in the composite membrane signifying high antibacterial activity of the membrane [28]. FE-SEM image (Figure 14(b)) confirmed highly porous structure of the composite membrane which aids in controlled release of the oil from the membrane [29].

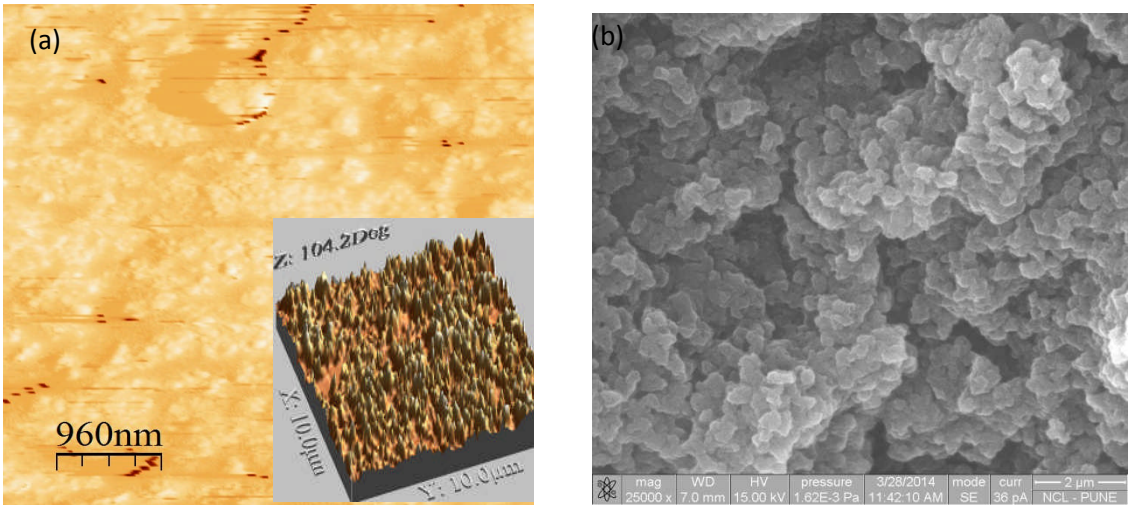

Figure 14: (a) 2D AFM & 3D AFM image (b) FE-SEM image of composite membrane

3.5 Significance of superhydrophilicity of the *Lantana*-PAN composite membrane

Figure 15 shows the images of phosphate buffer solution droplets on the surface of composite membrane attributing to superhydrophilic nature of the membrane. PAN itself is a hydrophobic material but this hydrophibicity is tailored to superhydrophilicity by homogenously mixing *Lantana camara* oil with dissolved PAN and converting it to membrane. Wetability of the composite surface was observed when volume of 8µL droplet of phosphate buffer solution (PBS) is dropped on the membrane surface. Quick wettability of the surface corresponds to the high surface energy of the composite membrane. Figure 11 (a-c) reveals the size of phosphate buffer droplet image on composite membrane during different time period. It is noted that time duration of shape of phosphate buffer droplet might provide the significance of superhydrophilic property of the composite membrane. During 1st second, droplet profile exhibits contact angle of 2˚ but during 2nd and 3rd second, droplet profile disappears/wets the surface, corresponding to superhydrophilic nature of composite membrane surface.

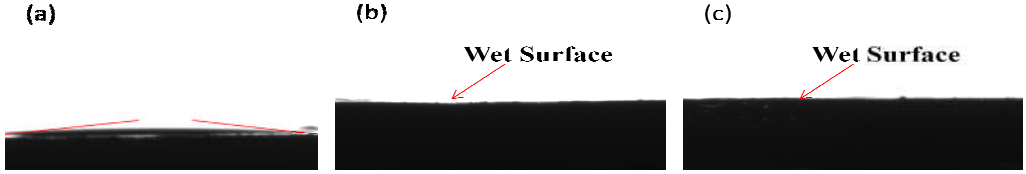

Figure 15: Contact angle measurement at (a) 1st sec (b) 2nd sec (c) 3rd sec

3.6 Antibacterial activity of composite membrane

Antibacterial efficacy of the composite membrane was monitored from the obtained zone of inhibition. Pristine PAN membrane was taken as control which exhibited no zone of inhibition. The *Lantana* oil-PAN composite membrane indicated enhanced antibacterial activity with 7-8 mm zone of inhibition of (Figure 16 1(a)) against Gram-negative bacteria and 8-10 mm zone against Gram-positive bacteria (Figure 16 1(b)) while zone of inhibition of oil alone against Gram-negative bacteria was 8-9 mm and 9-10 mm against Gram-positive bacteria (Figure 16 1(c)). Pyr-ADB-dialkyl-PAN composite membrane did not show any activity towards any bacteria indicating that synthetic repellents does not possess antibacterial activity (Figure 16 2(a) & (b)). The degree of inhibition zone in oil-PAN composite varies due to change in bacterial cell morphology. Gram-negative bacteria possess an extra lipopolysaccharide membrane (LPS) membrane over the outer membrane which provides the bacterium with a hydrophilic surface. This outer membrane serves as the penetration barrier against antibacterial agents which resists the hydrophobic antibiotics and toxic drugs [30]. The zone of inhibition of the bacterium remained unaltered for more than 30 day (Figure 17(a)) suggesting *Lantana* oil as the potential antibacterial agent. E-caryophyllene and germacrene D are the major volatile constituents of *Lantana camara* essential oil but E-caryophyllene is responsible for the antibacterial activity rather than germacrene D. *L. camara* plant from all habitats of the world is a well studied weed resulting in ranging volatile constituents depending on the niche. P. Weyerstahl et al. had clearly represented the main constituent of lantana oil from different countries indicating caryophyllene as one the main constituent found in all the countries [31]. Sonibare and Effiong investigated the antibacterial activity of L. camara found in Nigera resulted in β-caryophyllene instead of germacrene D as the major constituent of the oil responsible for antibacterial activity [32].

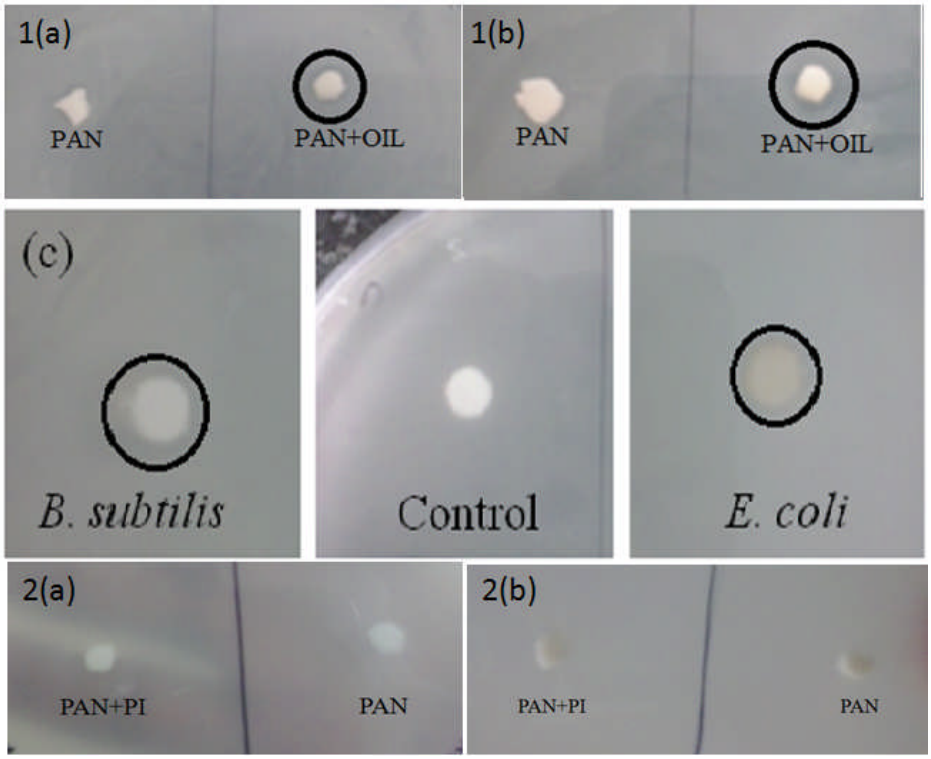

Figure 16: Zone of Inhibition against (1) OIL+PAN composite (a) *E. coli* (b) *Bacillus subtilis* (c) zone of inhibition of oil (2) PI+PAN composite (a) *E. coli* (b) *Bacillus subtilis*

3.7 *In-vitro* release study

In-vitro release study was performed in Phosphate buffer solution (PBS) (pH=7.4) to examine the sustained release of the bactericidal components from the composite membrane. Release of the oil from the membrane was monitored using UV-Vis spectrophotometer for 9 hr at 333 nm which exhibited pulsatile release profile (Figure 17(b)), a unique feature of particular drug. Pulsatile drug delivery system can be either site specific release or time dependent release. Site specific release is controlled by environmental factors such as pH/ enzyme whereas time dependent release is basically focussed on delivery time [33].

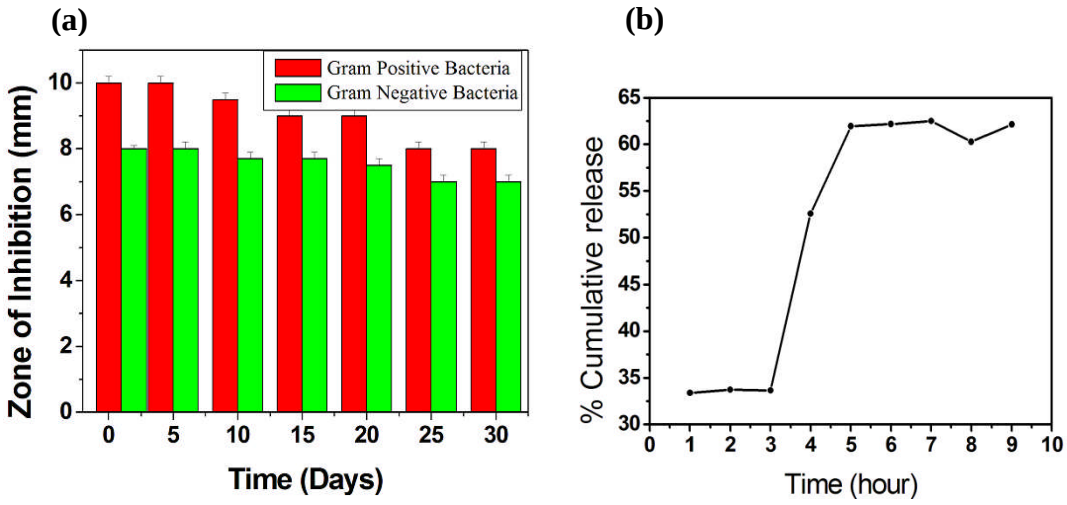

Figure 17: (a) Time dependent Zone of Inhibition (b) *In-vitro* release study of *Lantana* oil from the membrane

In the composite membrane PAN serves as a release-controlling agent. When exposed to aqueous media the polymeric membrane initially acts as a protective barrier and subsequently undergoes a timely failure based on diverse mechanisms depending on its physico-chemical and formulation characteristics. PAN is a semi-permeable membrane in which large quantity of oil is immobilised in amorphous regions and few in crystalline regions. The composite membrane swells in presence of water and an external water insoluble but permeable (as shown in FESEM image) polymer coating helps oil particle entrapped in the amorphous region to ooze out in the surrounding media instantaneously; whereas, the oil particles entrapped in crystalline region is released by diffusion into the surrounding medium. Lag time in pulsatile release is attributed to the gradual expansion or swelling of composite membrane, making it permeable thus allowing the drug molecule to diffuse outward (Figure 18). Since the cross sectional area remains constant as the membrane is swelled/eroded, the rate of release of oil from the core of the membrane remains constant.

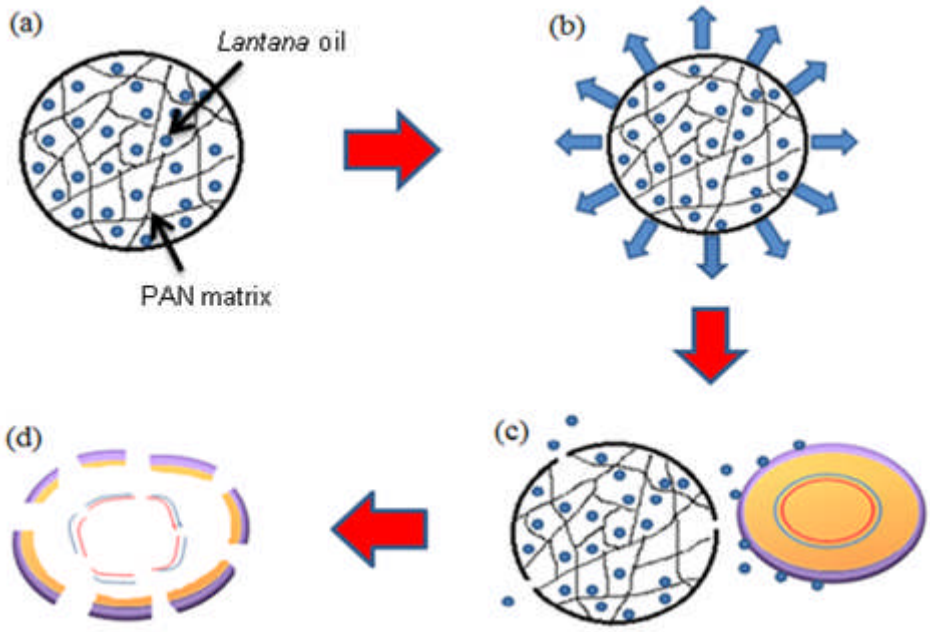

Figure 18: Schematic representation of bacterial death (a) *Lantana* oil-PAN composite membrane (b) swelling of membrane due to osmosis (c) attack of oil on bacterial cell (d) cell lysis

3.8 Cytotoxicity testing of composite membrane

The cytotoxicity of the composite membrane was assessed by mouse embryonic fibroblasts cell line (NIH 3T3) through MTT (yellow water soluble tetrazolium salt) assay [34] (Figure 19). More than 97% of cells were alive at 12.5 µg/mL while more than 91% of cells were alive at 200 µg/mL concentrations of sample; hence oil in the polymeric membrane is not toxic at even high concentrations. Succinate dehydrogenase, a mictochondrial enzyme in living cells cleaves the tetrazolium ring and converts the MTT to an insoluble purple formazan. Therefore, the amount of formazan produced is directly proportional to the number of viable cells [25]. Lidia et al. investigated the cytotoxic effect of *L. camara* essential oil in V79 mammalian cells. Essential oil induced considerable decrease in cell viability at concentration of 25 µg/mL and higher. This decrease in cell viability was attributed due to the presence of sesquiterpene, bicyclogermacrene, (+) spathulenol, trans- caryophyllene and sebinene [35]. While *Lantana camara*- PAN composite membrane works in favour of mouse embryonic fibroblast cell line (NIH 3T3), even at concentration of 25 µg/mL and 50 µg/mL shows 98% of cell viability, because the semi crystalline PAN membrane is restricting the oozing out of essential oil from the pores which thereby decreases the Cytotoxicity.

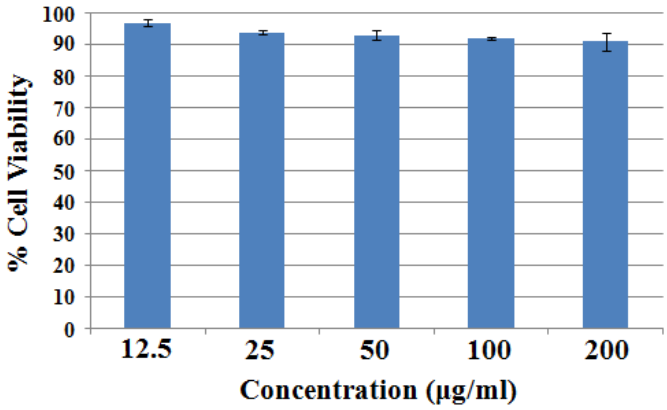

Figure 19: Cytotoxicity of *Lantana*-PAN composite membrane

3.9 Interaction between E-caryophyllene and PAN

When the *Lantana* oil is well dispersed in the PAN membrane, the interfacial interaction energy between the E-caryophyllene and polymer becomes very important in determining the antibacterial property of the composite membrane. The interaction energies ΔE between PAN and caryophyllene can be calculated as follows:

$$\Delta E = E_{PAN\text{-}caryophyllene} - (E_{caryophyllene} + E_{PAN}) \quad (2)$$

Where $E_{PAN\text{-}caryophyllene}$ is the potential energy of PAN/caryophyllene system, $E_{caryophyllene}$ is the potential energy of optimized caryophyllene moiety and E_{PAN} is the potential energy of optimized PAN polymer. The calculation of potential energy is based on the COMPASS force field. The potential energy E_{total} consists of three parts.

$$E_{total} = E_{valence} + E_{crossterms} + E_{non\text{-}bond} \quad (3)$$

Where $E_{valence}$, $E_{crossterms}$ and $E_{non\text{-}bond}$ is valence interaction energy, valence cross ters energy and non-bond interaction energy respectively.

Interaction energies between PAN and caryophyllene is calculate by Eq (2) and the result is listed in Table 1. In PAN-caryophyllene van der Wall, electrostatic and cross term interaction exists (Figure 20). No hydrogen bonding could be seen because of absence of strong electronegative groups on caryophyllene molecule.

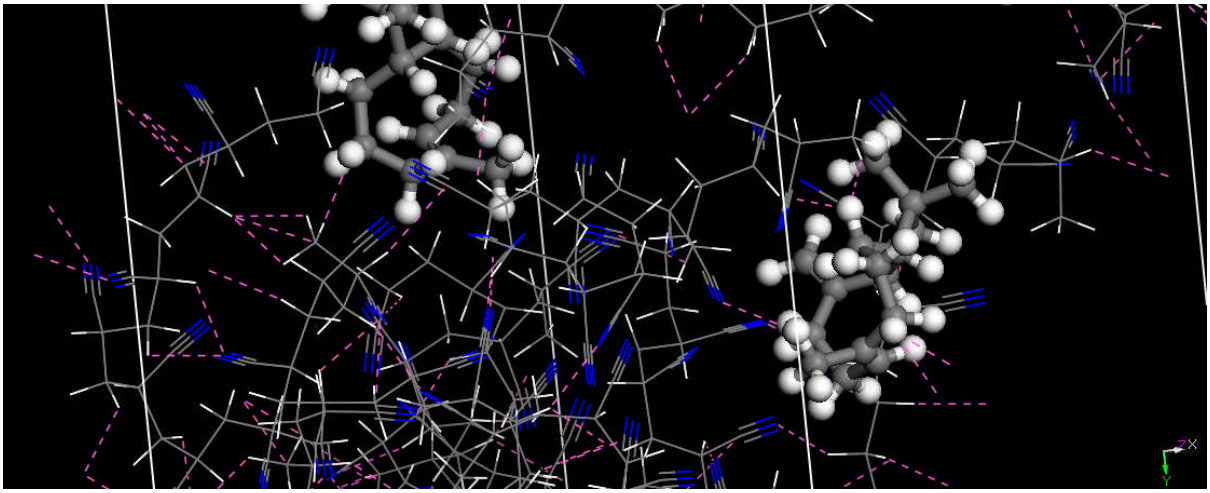

Figure 20: Simulated interactions between PAN and caryophyllene

Table 1: Interaction energies and Diffusion coefficients of PAN/caryophyllene system

	PAN/E-caryophyllene
ΔE_{Total} (kcal/mol)	-459.582
$\Delta E_{non\text{-}bond}$ (kcal/mol)	-84.381
$\Delta E_{valence}$ (kcal/mol)	-137.934
$\Delta E_{crossterm}$ (kcal/mol)	-237.267
Diffusion Coefficient (m^2/s)	$1.11*10^{-9}$

3.10 Diffusion Coefficient

Chain mobility which controls the diffusion paths constitutes a chief role in the transport properties of the antibacterial agent caryophyllene from the matrix during the release [36]. In this system, PAN is semi-crystalline polymer in which the mobility of the chains is constrained by the crystalline regions. Hence the chain mobility increases as there is increase in the disruption of crystalline region. Chain mobility is investigated by mean square displacement (MSD) of the chain as a function of simulation time. Figure 21 shows the MSDs of polymer chains which reveal the polymer chain mobility in the composite membrane. Diffusion studied of a molecule in the system could be calculated from the long-time limit of MSD by the Einstein relation [37]:

$$D = \frac{1}{6}\lim_{t\to\infty}\frac{d}{dt}\sum_{i=1}^{Na} < \left(r_i(t) - r_i(0)\right)^2 > \qquad (4)$$

Where D is the diffusion coefficient, r_i (t) and r_i (0) are the position of atom i at time t and 0, and the average is carried out over the region the time origin for

autocorrelation and over all the molecules as usual. The diffusion coefficient value is obtained from molecular dynamics simulation is listed in Table1. During the simulation, caryophyllene molecules were inserted into the membrane models. The diffusion runs were performed under the NVT conditions for 2 ns. The diffusion coefficient was an averaged value from all caryophyllene molecules.

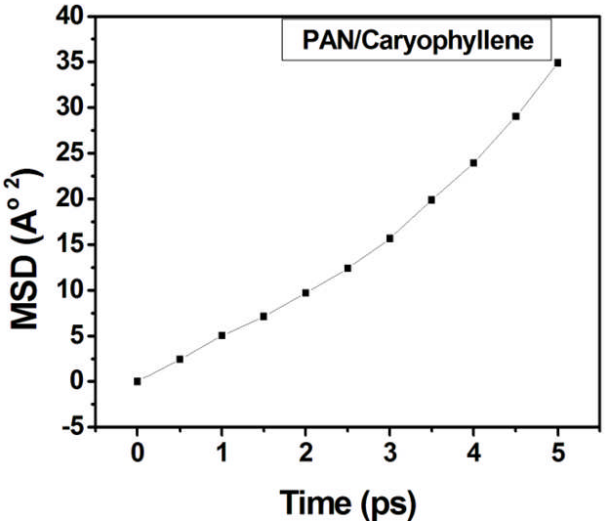

Figure 21: The MSDs of polymer chains in PAN containing caryophyllene

Free volume plays a major role in diffusion of the antibacterial agent from the polymeric membrane. The free volume is defined as the volume on the side of Connolly Surface without atoms. Free volume could be calculated experimentally through Positron annihilation lifetime spectroscopy (PALS) but this technique is very time consuming and does not gives exact details about the morphology of free volume voids. Hence simulation method is opted to characterize free volume theoretically [38]. Increased diffusion coefficient can be correlated with increase chain mobility and diffusion coefficient. Figure 22 shows the free volume voids in the optimized geometry of PAN/caryophyllene system. Free volume obtained through is listed in Table2. Since the free volume is less as compare to the total volume hence this could be attributed to the lag time in diffusion of caryophyllene from the PAN matrix as obtained experimentally through release study.

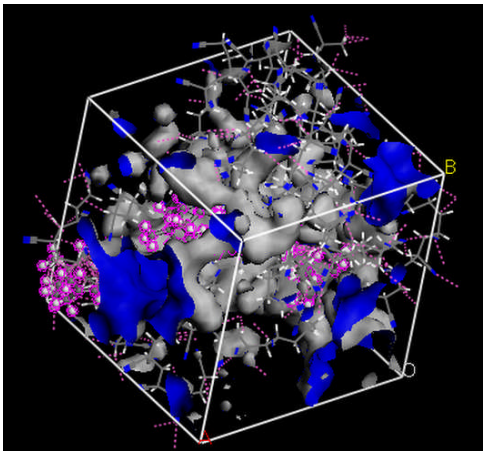

Figure 22: Simulated morphologies of free volumes (Shown in blue) in PAN/Caryophyllene system

Table 2: Free volume of PAN/caryophyllene system

	PAN/E-caryophyllene
Total Volume (A°^{3})	**7377.42**
Free Volume (A°^{3})	**2358.70**
Surface Area (A°^{2})	**2441.79**

3.11 Mosquito repellent activity

Since repellence assumes volatility of the active compounds hence Lantana camara essential oil was evaluated for its repellent activity. Different parts of plants contain a wide variety of complex chemical with unique biological activity which is thought to be cause by secondary metabolites including terpenoids, sesquiterpenoids, phenolics and alkaloids. Secondary metabolites present in different parts of plant contribute to bioefficacy such as ovicidal, repellency, insecticidal and antifeeding; monoterpenoids and sesquiterpenoids are mainly responsible for repellent activity [3940]. Lantana camara oil majorly constitutes of E-caryophyllene and germacrene D which are thought to be responsible for the mosquito repellent activity [41]. The oil was evaluated against *Aedes aegypti* at 0.25, 0.5, 0.75 and 1.5 mg/cm^2 concentrations (Table 3) by hand in cage experiment. At 1.5 mg/cm^2, essential oil offered 100% protection time for 8 h 30 min while DEET offered 100% protection for more than 9 h at 0.5 mg/cm^2.

Table 3: Mosquito repellent activity of *Lantana* oil and synthetic repellents

SAMPLE	PROTECTION TIME OFFERED (in hours)			
Concentration (mg/cm^2)	0.25	0.5	0.75	1.5
OIL	0.35 ± 0.05	1.16 ± 0.16	2.21 ± 0.14	8.5 ± 0.28
PE	No Activity	No Activity	No Activity	No Activity
PI	3.26 ± 0.14	8 ± 0.28	-	-
PB	No Activity	No Activity	No Activity	1.8 ± 0.19
PH	No Activity	No Activity	No Activity	No Activity
DEET (Control)	8.25 ± 0.14	>9.5 ± 0.28	-	-

Pyr-ADB derivatives were also evaluated against *Aedes aegypti* at 0.25, 0.5, 0.75 and 1.5 mg/cm^2 concentrations (Table 3) by hand in cage experiment. In the preliminary assay for the minimum effective dose (MED), Pyr-ADB-diisopropyl (PI) (MED 0.25 mg/cm^2) showed almost half level of activity to that of DEET at the same MED while the activity became almost comparable to DEET at MED of 0.5 mg/cm^2. The control acetone was not repellent. PE and PH does not show any activity even at high concentrations but PB showed repellency of 1.8 h at a very high concentration of 1.5 mg/cm^2 which is beyond consideration because of the high concentration. All the Pyr-ADB derivatives differ in the alkyl chain; hence alkyl chain is playing a crucial role in the mosquito repellency. PE, PB and PH contain a linear chain while PI has got a branching chain which is thought to be responsible for the repellent activity. Due to branching in the chain of PI it becomes slightly more hindered and less flexible which it to fit properly in the cavity of olfactory receptor neuron and hence inhibiting the attracting tendency of mosquitoes towards human emanations. Amides have been a highly potential group in most of the repellents since past 50 year because of the van der Waals surfaces, electrostatic potential, dipole moments and charge on amide nitrogen. All the above mentioned secondary forces makes amide an evergreen group as a repellent [14]. Some of the promising branched mosquito repellents are MGK 264, MGK 326 and ethyl N-acetyl-N-butyl-3-aminopropionate (IR3535). Katritzky et al. investigated several molecules for their repellent efficacy thorough a model of Artificial Neural Network (ANN) resulting that 1-(1-azepanyl)-1-hexanone was the most potential carboxamide with MED equal to that of DEET (0.047±0.007 µmol/cm^2) while (E)-1-(1-azepanyl)-2-methyl-2-penten-1-one, 1-(1-azepanyl)-2-methyl-1-pentenone and N-butyl-N-ethyl-2-methylpentanamide were inferior to DEET in terms of repellency despite of high MED [24].

Conclusions

This particular thesis aimed to find out novel synthetic and botanical mosquito repellents. In this regard we have chosen dicarboxamide derivatives of Pyr-ADB-dialkyl which were synthesized using short and efficient synthetic steps reactions. Among the four repellents synthesized Pyr-ADB-diisopropyl (PI) showed good results with repellent activity of 8 h comparable to that of DEET at MED of 0.5 mg/cm^2 while *Lantana camara* oil (botanical repellent) showed similar amount of repellent activity i.e. of 8.5 h at MED of 1.5 mg/cm^2. Hence both *Lantana* oil and Pry-ADB-diisopropyl could be used as an effective mosquito repellent in forms of creams, lotions, fibres, patches etc. in future.

Lantana oil is also an effective antimicrobial agent and upon encapsulation oil in polyacrylonitrile (PAN) membrane pulsatile release was observed which is an unique feature for any drug and has got efficient medical application as various diseases require pulsatile behaviour of drug for effective healing. The zone of inhibition against *E. coli* and *B. subtilis* was observed to be 7-8 mm and 8-10 mm while the zone of inhibition of oil alone was observed to be 8-9 mm and 9-11 mm respectively. Morphometric studies of oil-PAN composite membrane was done by AFM and FESEM revealing the porous structure of the membrane which helps in oozing out of oil from the membrane. Superhydrophilicity of the membrane was confirmed by drop shape analysis system. The modelling studies showed small free volume and diffusion coefficient which is considered a reason of 3 h lag time in release of cryophyllene from PAN matrix. This result is extensively supported by experimentally obtained result for release study. Biocompatibility of the composite membrane was studied by MTT assay exhibiting 97% viable cells at concentration of 12.5 µg/mL and 92% viable cells at 200 µg/mL. Such *Lantana camara*-PAN membranes can find wide applications in time dependent drug release systems and as water filtration resulting in pathogen free drinking water.

References

[1] Gupta, R. K.; Rutledge, L. C. Role of repellents in vector control and disease prevention. *Am. J. Trop. Med. Hyg.*, **1994**, 50, 82–86.

[2] Lane, R. P.; Crosskey, R. W. Medical Insects and Arachnids. Chapman and Hall publisher, 1993**.**

[3] Edman, J.; Eldridge, B.F. Medical Entomology - A Textbook on Public Health and Veterinary Problems Caused by Arthropods. Kluwer academic publisher, 2004.

[4] Rozendaal, J. A. Mosquitos and other biting Diptera. In vector control," *WorldHealth Organ.* **1997**, 5–177.

[5] Manguin, S.; Bangs, M. J.; Pothikasikorn, J.; Chareonviriyaphap, T. Review on global co-transmission of human Plasmodium species and Wuchereria bancrofti by Anopheles mosquitoes. *Infect. Genet. Evol.* **2010**, 10, 159–177.

[6] Renault, P.; Solet, J.-L.; Sissoko, D.; Balleydier, E.; Larrieu, S.; Filleul, L.; Lassalle, C.; Thiria, J.; Rachou, E.; Valk, H. de; Ilef, D.; Ledrans, M.; Quatresous, I.; Quenel, P.; Pierre, V. A Major Epidemic of Chikungunya Virus Infection on Reunion Island, France, 2005- 2006. *Am J Trop Med Hyg* **2007**, 77, 727–731.

[7] "Blackwell, A.; Stuart, A.E; Estambale, B.A. The repellent and antifeedant activity of Myrica Gale oil against Aedes aegypti mosquitoes and its enhancement by the addition of salicyluric acid. *J.R. Coll. Physicians Edinb*, **2003**, 33: 209.

[8] Takken, W.; Knols, B. G. Odor-mediated behavior of Afrotropical malaria mosquitoes. *Annu. Rev. Entomol.* **1999**, 44, 131–157.

[9] Padilha de Paula, J.; Gomes-Carneiro, M. R.; Paumgartten, F. J. R. Chemical composition, toxicity and mosquito repellency of Ocimum selloi oil. *J. Ethnopharmacol.* **2003**, 88, 253–260.

[10] Sukumar, K.; M. Perich, J., Boobar, L. R. Botanical derivatives in mosquito control: a review. *J. Am. Mosq. Control Assoc.* **1991**, 7, 210–237.

[11] Davis, E. M.; Croteau, R. Cyclization Enzymes in the Biosynthesis of Monoterpenes , Sesquiterpenes , and Diterpenes. *Top. Curr. Chem.* **2000**, 209, 53–95.

[12] Regnault-Roger, C.; Vincent, C.; Arnason, J. T. Essential oils in insect control: low-risk products in a high-stakes world. *Annu. Rev. Entomol.* **2012**, 57, 405–424.

[13] WHO, Report of the WHO informal consultation on the evaluation ad testing of insecticides. Geneva, 1996 .

[14] Paluch, G.; Bartholomay, L.; Coats, J. Mosquito repellents : a review of chemical structure diversity and olfaction. *Pest Manag. Sci.* **2010**, 66, 925–935.

[15] Ellin, R. I.; Farrand, R. L.; Oberst, F. W.; Crouse, C. L.; Billups, N. B.; Koon, W. S.; Musselman, N. P.; Sidell, F. R. An apparatus for the detected and quantitation of volatile human effluents. *J. Chromatogr. A* **1974**, 100, 137–152.

[16] Brennan, N. K.; Donnelly, D. J.; Detty, M. R. Selenoxanthones via directed metalations in 2-arylselenobenzamide derivatives. *J. Org. Chem.* **2003**, 68, 3344–3347.

[17] Diedrich, C. L.; Haase, D.; Saak, W.; Christoffers J. Regioselectivity of Friedländer Quinoline Syntheses. *European J. Org. Chem.* **2008**, 10, 1811–1816.

[18] Yadav, R.; Kandasubramanian, B. Egg albumin PVA hybrid membranes for antibacterial application. *Mater. Lett.* 2013, 110, 130–133.

[19] Cheesman, B. T.; Neilson, A. J. G.; Willott, J. D.; Webber, G. B.; Edmondson, S.; Wanless, E. J. Effect of colloidal substrate curvature on pH-responsive polyelectrolyte brush growth. *Langmuir* **2013**, 29, 6131–6140.

[20] Wang, L.; Liu, F.; Jiang, Y.; Chai, Z.; Li, P.; Cheng, Y.; Jing, H.; Leng, X. Synergistic antimicrobial activities of natural essential oils with chitosan films. *J. Agri. Food Chem.* **2011**, 59, 12411–12419.

[21] Parris, N.; Cooke, P. H.; Hicks, K. B. Encapsulation of essential oils in zein nanospherical particles. *J. Agri. Food Chem.* **2005**, 53, 4788–4792.

[22] Mosmann, T. Rapid colorimetric assay for cellular growth and survival: Application to proliferation and cytotoxicity assays. *J. Immunol. Methods* **1983**, 65, 55–63.

[23] Sun, H. Ab initio calculations and force field development for computer simulation of polysilanes. *Macromolecules* **1995**, 28, 701–712.

[24] Katritzky, A. R.; Wang, Z.; Slavov, S.; Dobchev, D.; Hall, C. D.; Tsikolia, M.; Bernier, U. R.; Elejalde, N. M.; Clark, G. G.; Linthicum, K. J. Novel carboxamides as potential mosquito repellents. *J. Med. Entomol.* **2010**, 47, 924–938.

[25] Schreck, C. E. Techniques for the evaluation of insect review repellents:A critical review. *Ann. Rev.Entomol.* **1977**, 27, 101-119.

[26] Deans, S. G.; Ritchie, G. Antibacterial properties of plant essential oils," *Int. J. Food Microbiol.* **1987**, 5, 165–180.

[27] Sabrish, B.; Sahoo, B.N.; Kandasubramanian, B. Controlled anisotropic wetting behaviour of multi-scale slippery surface structure of non fluoro polymer composite. *Express Polym. Lett.* **2013**, 7, 900–909.

[28] Pal, S.; Tak, Y. K.; Song, J. M. Does the antibacterial activity of silver nanoparticles depend on the shape of the nanoparticle? A study of the Gram-negative bacterium Escherichia coli. *Appl. Environ. Microbiol.* **2007**, 73, 1712–1720.

[29] Zhang, L.; Luo, J., Menkhaus, T. J.; Varadaraju, H.; Sun, Y.; Fong H. Antimicrobial nano-fibrous membranes developed from electrospun polyacrylonitrile nanofibers. *J. Memb. Sci.* **2011**, 369, 499–505.

[30] Kong, M.; Chen, X. G.; Xing, K.; Park, H. J. Antimicrobial properties of chitosan and mode of action: a state of the art review. *Int. J. Food Microbiol.* **2010**, 144, 51–63.

[31] Weyerstahl P.; Marschall, H.; Eckhardt, A.; Christiansen, C. Constituents of commercial Brazilian lantana oil. *J. Flavour Fragr.* **1999**, 28, 15–28.

[32] Sonibare, O. O.; Effiong, I. Antibacterial activity and cytotoxicity of essential oil of Lantana Camara L . leaves from Nigeria. *African J. Biotechnol.* **2008**, 7, 2618–2620.

[33] Bussemer, T.; Otto, I.; Bodmeier, R. Pulsatile drug-delivery systems. *Crit. Rev. Ther. Drug Carrier Syst.* **2001**, 18, 433–58.

[34] Kandasubramanian, B.; Govindaraj, P. Peeling model for cell adhesion on electrospun polymer nanofibres. *J. Adhes. Sci. Technol.* **2014**, 28, 171–185.

[35] Medeiros, L. B. P.; Rocha, M. dos S.; Lima, S. G. de; Júnior, G. R. de S.; Citó, A. M. das G. L.; Da, D. S.; Lopes, J. A. D.; Moura, D. J.; Saffi, J.; Mobin, M.; da Costa, J. G. M. Chemical constituents and evaluation of cytotoxic and antifungal activity of Lantana camara essential oils. *Brazilian J. Pharmacogn.* **2010**, 22, 1259–1267.

[36] Nagel, C.; Schmidtke, E.; Günther-Schade, K.; Hofmann, D.; Fritsch, D.; Strunskus, T.; Faupel, F. Free Volume Distributions in Glassy Polymer Membranes: Comparison between Molecular Modeling and Experiments. *Macromolecules* **2000**, 33, 2242–2248.

[37] Feng, H.; Gao, W.; Sun, Z.; Lei, B.; Li, G.; Chen, L. Molecular Dynamics Simulation of Di ff usion and Structure of Some n - Alkanes in near Critical and Supercritical Carbon Dioxide at In fi nite Dilution *J. Phys. Chem. B* **2013**, 117, 12525–12534.

[38] Pan, F.; Peng, F.; Lu, L.; Wang, J.; Jiang, Z. Molecular simulation on penetrants diffusion at the interface region of organic–inorganic hybrid membranes. *Chem. Eng. Sci.* **2008**, 63, 1072–1080.

[39] Chang, K.-S.; Tak, J.-H.; Kim, S.-I.; Lee, W.-J.; Ahn, Y.-J. Repellency of Cinnamomum cassia bark compounds and cream containing cassia oil to Aedes aegypti (Diptera: Culicidae) under laboratory and indoor conditions. *Pest Manag. Sci.* **2006**, 62, 1032–1038.

[40] Grayson, D. H. Monoterpenoids (mid-1997 to mid-1999). *Nat. Prod. Rep.* **2000**, 17, 385–419.

[41] Fraga, B. M. Natural sesquiterpenoids. *Nat. Prod. Rep.* **2010**, 27, 1681–1708.

.